Analysis of Oxysterols by Electrospray Tandem Mass Spectrometry

William J. Griffiths and Yuqin Wang
Department of Pharmaceutical and Biological Chemistry, The School of Pharmacy, University of London, London, United Kingdom

Gunvor Alvelius, Suya Liu, Karl Bodin, and Jan Sjövall
Department of Medical Biochemistry and Biophysics, Karolinska Institutet, Stockholm, Sweden

Oxysterols are oxygenated derivatives of cholesterol. They are intermediates in cholesterol excretion pathways and may also be regarded as transport forms of cholesterol. The introduction of additional hydroxyl groups to the cholesterol skeleton facilitates the flux of oxysterols across the blood brain barrier, and oxysterols have been implicated in mediating a number of cholesterol-induced metabolic effects. Oxysterols are difficult to analyze by atmospheric pressure ionization mass spectrometry on account of the absence of basic or acidic functional groups in their structures. In this communication, we report a method for the derivatization and analysis of oxysterols by electrospray mass spectrometry. Oxysterols with a 3β-hydroxy-Δ^5 structure were converted by cholesterol oxidase to 3-oxo-Δ^4 steroids and then derivatized with the Girard P reagent to give Girard P hydrazones, which were subsequently analyzed by tandem mass spectrometry. The improvement in sensitivity for the analysis of 25-hydroxycholesterol upon oxidation and derivatization was over 1000.   (J Am Soc Mass Spectrom 2006, 17, 341–362) © 2006 American Society for Mass Spectrometry

The introduction of an oxygen function in the cholesterol (C^5-3β-ol) molecule with the formation of an oxysterol is the first step in cholesterol degradation pathways [1, 2]. The quantitatively most important catabolic pathway is the subsequent conversion of the oxysterol into water-soluble bile acids. However, other oxysterols are intermediates in the formation of steroid hormones. Oxysterol formation can occur in many tissues and organs, and conversion of an oxysterol to a bile acid is not restricted to the liver [3–7]. Hormonally active steroids can also be synthesized from cholesterol outside the endocrine organs. Some oxysterols are ligands to nuclear receptors, e.g., the liver X receptor (LXR) α and β, and are considered to have important roles in the regulation of cholesterol and lipid metabolism and homeostasis [8–15]. Some oxysterols have been proposed to mediate inflammatory events in the development of atherosclerotic lesions [16]. A variety of oxysterols are found in blood and tissues, exemplified by 27-hydroxycholesterol (C^5-3β,27-diol), 7α-hydroxycholesterol (C^5-3β,7α-diol), 24S-hydroxycholesterol (C^5-3β,24S-diol), and 4β-hydroxycholesterol (C^5-3β,4β-diol) (see Scheme 1 for steroid skeleton and numbering system). The levels in plasma of healthy subjects vary between about 30 and 150 ng/mL. Minor oxysterols include 25-hydroxycholesterol (C^5-3β,25-diol), 7β-hydroxycholesterol (C^5-3β,7β-diol), 7-oxocholesterol (C^5-3β-ol-7-one), cholesterol-5,6-epoxides (C-3β-ol-5,6-epoxide), cholestane-3,5,6-triols (C-3β,5,6-triol) [2]. The levels of these compounds are usually below 10 ng/mL. Other oxysterols that have been found, e.g. in brain, include 20-hydroxycholesterol (C^5-3β,20-diol) and 22-hydroxycholesterol (C^5-3β,22-diol) [17, 18]. There is always some doubt with respect to the origin of the minor oxysterols as they can be formed by non-enzymatic oxidation of cholesterol [2]. Oxysterols are present in only trace amounts in biological systems, where the excess of cholesterol is invariably more than three orders of magnitude.

Oxysterols with a 3β,7α-dihydroxy-5-ene structure can be oxidized to the corresponding 7α-hydroxy-4-en-3-ones, and 27-hydroxylated oxysterols can be converted to 27-carboxylic acids both in the liver and extrahepatically. Examples of such metabolites occurring in human circulation are 7α-hydroxycholest-4-en-3-one (C^4-7α-ol-3-one), 3β-hydroxycholest-5-en-27-oic acid (CA^5-3β-ol), 3β,7α-dihydroxycholest-5-en-27-oic acid (CA^5-3β,7α-diol), and 7α-hydroxy-3-oxo-cholest-4-en-27-oic acid (CA^4-7α-ol-3-one) (Scheme 1). Because of their structures and since some of them have regulatory

Scheme 1. Nuclear skeletons and side-chain structures on which sterols and oxysterols are based. For example, in cholesterol (C[5]-3β-ol) the side-chain R_1 is attached to the 3β-hydroxy-Δ^5 nucleus; in 3β-hydroxycholest-5-en-27-oic acid (CA[5]-3β-ol) the side-chain R_2 is attached to the 3β-hydroxy-Δ^5 nucleus; in cholest-4-en-3-one (C[4]-3-one) the side-chain R_1 is attached to the 3-oxo-Δ^4 nucleus, in 3β-hydroxychol-5-en-24-oic acid (BA[5]-3β-ol) the side-chain R_3 is attached to the 3β-hydroxy-Δ^5 nucleus; and in 3β-hydroxy-5-oxo-5,6-secocholestan-6-al (5,6-seco-sterol) R_1 is attached to the 3β-hydroxy-5-oxo-5,6-seco-6-al nucleus. The C_{24} bile acid side-chain is shown for comparison.

properties similar to those of the conventional oxysterols [19] (or bind to nuclear receptors), it is logical to extend the term oxysterol to include these types of compounds.

Oxysterols are widely distributed in tissues and cells. Their localization is partly related to their structures and sites of formation. For example, 7α-hydroxycholesterol is exclusively formed in the liver by the action of CYP7A1. Its formation is the regulated, rate-limiting step in bile acid biosynthesis and the levels of 7α-hydroxycholesterol and 7α-hydroxycholest-4-en-3-one in the circulation are positively correlated to the activity of CYP7A1 in the liver [20–22]. 27-Hydroxycholesterol, the quantitatively dominant oxysterol in the circulation of adult humans (~120 ng/mL plasma) is formed by the action of CYP27A1 which has a broad substrate specificity and is present in most tissues [1, 2]. The 3β-hydroxycholest-5-en-27-oic acid in human plasma

(formed from 27-hydroxycholesterol [23]) originates mostly from the lung [7]. 24S-Hydroxycholesterol in the human circulation originates mainly from the brain, where it is formed by the action of CYP46A1 [24]. While 7α-hydroxycholesterol, 27-hydroxycholesterol and 3β-hydroxycholest-5-en-27-oic acid are efficiently converted into bile acids in the liver, about half of the 24S-hydroxycholesterol formed in humans is excreted in bile in a sulphated or glucuronidated form. This illustrates that oxysterols, besides being in the free form (and as fatty acid esters), can occur in different conjugated forms. It has been shown recently that that 24S-hydroxycholesterol can be further metabolized into 24,27-dihydroxycholesterol (C[5]-3β,24,27-triol) in man [25]. 4β-Hydroxycholesterol is formed by the action of CYP3A4 [26], the major cytochrome P450 in human liver. The metabolic end products of 4β-hydroxycholesterol have yet to be defined.

Besides known naturally occurring oxysterols, a large number of synthetic oxysterols have been shown to be potential ligands to nuclear receptors. It is not known if some of these occur naturally, and there is a need for methods to make comprehensive studies of the nature and levels of oxysterols in tissues and body fluids. This is illustrated by the recent identification of novel oxysterols, formed from cholesterol by the action of ozone, in human tissues [27–30]. Evidence has been presented for their involvement in the mediation of inflammatory processes associated with the development of atherosclerotic lesions [28], and in the initiation of protein misfolding as occurs in several neurological diseases [29]. Of these products, 3β-hydroxy-5-oxo-5,6-secocholestan-6-al (5,6-seco-sterol), a ketoaldehyde, and its aldol condensation product both contain a reactive aldehyde group (Scheme **1**). Incubation of 5,6-seco-sterol, or its aldol, with amyloid β peptide (Aβ) leads to amyloidogenesis, possibly by condensation with amino groups in the peptide [29]. The levels of the 5,6-seco-sterol and its aldol were surprisingly high in brain of patients with Alzheimer's disease and healthy subjects [combined seco-sterol levels ~0.44 pmol/mg (~180 ng/g) and ~0.35 pmol/mg (~150 ng/g), respectively]. Biologically active oxysterols are also formed during ozonolysis of cholesterol in lung surfactant [30]. Pulfer and Murphy [30] identified the major cholesterol derived ozonolysis product in lung surfactant as 5β,6β-epoxycholesterol (C-3β-ol-5β,6β-epoxide). In studies of the metabolism of this oxysterol in lung epithelial cells they found small amounts of the expected metabolite cholestane-3β, 5α, 6β-triol (C-3β, 5α, 6β-triol), and more abundant levels of the unexpected metabolite 3β, 5α-dihydroxycholestan-6-one (C-3β, 5α-diol-6-one). Significantly, both 5β, 6β-epoxycholesterol and 3β, 5α-dihydroxycholestan-6-one were shown to be cytotoxic to human bronchial epithelial cells.

Traditionally, oxysterols have been analyzed by isotope-dilution gas-chromatography-mass spectrometry (GC-MS) [31, 32]. However, high-performance liquid chromatography (HPLC) methods have been intro-

duced in which oxysterols are converted to their 3-oxo-Δ^4 derivatives which are then analyzed and detected using their UV chromophore at 205-210 or 240 nm [33, 34]. In the current study, we have followed an analogous methodology whereby steroids with a 3β-hydroxy-Δ^5 structure have been converted to their 3-oxo-Δ^4 oxidation products by treatment with cholesterol oxidase [35–37], and then reacted with Girard P (GP) reagent to give GP hydrazones [38, 39]. Girard hydrazones possess a quaternary nitrogen and are readily analyzed by electrospray (ES) mass spectrometry [35–45]. Furthermore, tandem mass spectrometry (MS/MS) provides high sensitivity and structural information for GP hydrazone analysis. Griffiths et al. were able to obtain structurally informative ES-MS/MS spectra for steroid GP hydrazones from sub-pg quantities of sample [38, 39]. In the current study we have explored the MS/MS fragmentation patterns of a series of oxysterol GP hydrazones, and evaluated the potential of these derivatives for analyzing oxysterols in biological samples. We have also optimized the enzymatic conversion of oxysterols to their 3-oxo-Δ^4 analogs under conditions compatible with subsequent ES analysis, and also optimized the derivatization reaction so as to be suitable for labile steroids, i.e., 7-hydroxy-Δ^4-3-oxo-steroids. The methodology was tested in an analysis of an oxysterol fraction from rat brain.

Experimental

Materials

Solvents were of analytical grade. Water was from a Milli-Q water system (Millipore, Molsheim, France). The oxysterols 7β-hydroxycholesterol, 24S-hydroxycholesterol, 20R,22R-dihydroxycholesterol (C^5-3β,20R,22R-triol), and 22-oxocholesterol (C^5-3β-ol-22-one) were kind gifts from Professor I. Björkhem of the Division of Clinical Chemistry, Karolinska Institutet. Other oxysterols and steroids, i.e., 25-hydroxycholesterol, 27-hydroxycholesterol, [16,16,17(or 20),22,22,23,23-^{2}H$_7$]27-hydroxycholesterol ([^{2}H$_7$]C^5-3β,27-diol), 7α,25-dihydroxycholesterol (C^5-3β,7α,25-triol), 7β,25-dihydroxycholesterol (C^5-3β,7β,25-triol), 7α,27-dihydroxycholesterol (C^5-3β,7α,27-triol), [16,16,17(or 20),22,22,23,23-^{2}H$_7$] 7α,27-dihydroxycholesterol ([^{2}H$_7$]C^5-3β,7α,27-triol), [16,16,17(or 20),22,22,23,23-^{2}H$_7$] 3β-hydroxycholest-5-en-27-oic acid ([^{2}H$_7$]CA^5-3β-ol), [16,16,17(or 20),22,22,23,23-^{2}H$_7$] 3β,7α-dihydroxycholest-5-en-27-oic acid ([^{2}H$_7$]CA^5-3β,7α-diol), [16,16,17(or 20), 22,22,23,23-^{2}H$_7$] 3β,7α-dihydroxycholest-5-en-27-oic acid methyl ester ([^{2}H$_7$]CA^5-3β,7α-diol-27-methyl ester), 3β,7β-dihydroxycholest-5-en-27-oic acid (CA^5-3β,7β-diol), 3β-hydroxychol-5-en-24-oic acid (BA^5-3β-ol), [2,2,4,4,23-^{2}H$_5$] 3β-hydroxychol-5-en-24-oic acid ([^{2}H$_5$]BA^5-3β-ol), 3β,7α-dihydroxychol-5-en-24-oic acid (BA^5-3β,7α-diol), [2,2,4, 4,23-^{2}H$_5$] 3β-hydroxychol-5-en-24-oylglycine ([^{2}H$_4$]BA^5-3β-ol-24-oylglycine), cholesterol (C^5-3β-ol), desmosterol (C^{5,24}-3β-ol), sitosterol (C^5-24β-ethyl-3β-ol), stigmasterol (C^{5,22}-24β-ethyl-3β-ol), testosterone (A^4-17β-ol-3-one), and

[19,19,19-^{2}H$_3$] testosterone were from previous studies in the Karolinska laboratory (Table 1) [38, 39, 46].

Oxidation of 3β-Hydroxy-Δ^5 Sterols to 3-Oxo-Δ^4 Sterols

The 3β-hydroxy-Δ^5 sterols (and bile acids and steroids) were oxidized with cholesterol oxidase essentially as described by Brooks et al. [47]. Recombinant, lyophilized, cholesterol oxidase from *Brevibacterium* was obtained from Roche Diagnostics GmbH, Mannheim, Germany, through the courtesy of Dr. Ingo Preuss. The enzyme from *Brevibacterium* was selected since, in contrast to the common enzyme from *Nocardia*, it also catalyzes the oxidation of 3β-hydroxy-Δ^5 steroids of the C$_{19}$ and C$_{21}$ series [48]. Steroids of the latter type are important intermediates in steroid hormone biosynthesis with biological functions, e.g., as neurosteroids in brain [49, 50]. The 3β-hydroxy-Δ^5 sterols (1 μg) were dissolved in 50 μL of isopropanol, and 10 μL of cholesterol oxidase (1 mg/mL, 20U/mg protein) in 1 mL of buffer (50 mM KH$_2$PO$_4$, pH 7) was added; the mixture was incubated at room temperature (25 °C for 2 to 12 h) and subsequently used as the starting solution for reaction with the GP reagent as described below. In initial experiments designed to study the extent of the oxidation reaction (primarily using bile acids), the enzyme reaction was stopped after overnight incubation by the addition of 1 mL of methanol, and passed through a Sep-Pak C$_{18}$ cartridge (100 mg, Waters, Milford, MA) prepared in water. The effluent and a 1 mL water-wash were combined and passed again through the same Sep-Pak cartridge. After washing with 1 mL of 20% methanol the 3-oxo-Δ^4 sterols were eluted with 2 × 1 mL of methanol, and 1 mL chloroform/methanol, 1:1 (vol/vol), if needed.

Derivatization of Oxosterols

The derivatization of oxosterols to GP hydrazones was carried out essentially as described by Shackleton et al. [40] and by Wheeler [51]. The reaction mixture from the oxidation step above was used directly after the incubation without any further treatment. The oxidation mixture, 1 mL (50 mM phosphate buffer, 5% isopropanol, 10 μg enzyme and 1 μg sterols) was diluted with 2 mL of methanol to give a 70% methanol solution, and 150 mg of GP hydrazine (Sigma-Aldrich, Poole, Dorset, UK) and 150 μL of glacial acetic acid were added. The mixture was left at room temperature overnight.

In initial studies, when the derivatization reaction was applied to reference compounds, the next step was to dry the steroid GP hydrazone under a stream of nitrogen gas and reconstitute in a solution of 10% aqueous methanol (1 mL). The steroid GP hydrazone was then separated from excess reagent by extraction on a Sep-Pak C$_{18}$ cartridge. After washing with 10%

Table 1. Steroids and oxysterols analyzed as GP hydrazones

Name	Abbreviation	Oxidation product	Mass of GP	Cmpd (MS/MS Fig[4])
Cholesterol	C^5-3β-ol	C^4-3-one	518.41	I (3c)
Desmosterol	$C^{5,24}$-3β-ol	$C^{4,24}$-3-one	516.40	II (S-4b)
Sitosterol	C^5-24β-ethyl-3β-ol	C^4-24β-ethyl-3-one	546.44	III (S-4c)
Stigmasterol	$C^{5,22}$-24β-ethyl-3β-ol	$C^{4,22}$-24β-ethyl-3-one	544.43	IV (S-4d)
7β-hydroxycholesterol	C^5-3β,7β-diol	C^4-7β-ol-3-one	534.41	V (2e)
24-hydroxycholesterol	C^5-3β,24-diol	C^4-24-ol-3-one	534.41	VI (2a)
25-hydroxycholesterol	C^5-3β,25-diol	C^4-25-ol-3-one	534.41	VII (2c)
27-hydroxycholesterol	C^5-3β,27-diol	C^4-27-ol-3-one	534.41	VIII (2d)
[16,16,17(or20),22,22,23, 23-^{2}H$_7$] 27-hydroxycholesterol	[16,16,17(or20),22,22,23, 23-^{2}H$_7$]C^5-3β,27-diol	[16,16,17(or20),22,22,23, 23-^{2}H$_7$]C^4-27-ol-3-one	541.45	IX
22-oxocholesterol	C^5-3β-ol-22-one	C^4-3,22-dione	532.39[1]	X (2f)
22-oxocholesterol	C^5-3β-ol-22-one	C^4-3,22-dione	666.46[2]	XI (2g)
20R,22R-dihydroxycholesterol	C^5-3β,20R,22R-triol	C^4-20R,22R-diol-3-one	550.40	XII (3b)
7α,25-dihydroxycholesterol	C^5-3β,7α,25-triol	C^4-7α,25-diol-3-one	550.40	XIII (S-1c)
7β,25-dihydroxycholesterol	C^5-3β,7β,25-triol	C^4-7β,25-diol-3-one	550.40	XIV (S-1d)
7α,27-dihydroxycholesterol	C^5-3β,7α,27-triol	C^4-7α,27-diol-3-one	550.40	XV (3a)
[16,16,17(or20),22,22,23, 23-^{2}H$_7$] 7α,27-dihydroxycholesterol	[16,16,17(or20),22,22,23, 23-^{2}H$_7$]C^5-3β,7α,27-triol	[16,16,17(or20),22,22,23, 23-^{2}H$_7$]C^4-7α,27-diol-3-one	557.44	XVI (S-1b)
[16,16,17(or20),22,22,23, 23-^{2}H$_7$] 3β-hydroxycholest-5-en-27-oic acid	[16,16,17(or20),22,22,23, 23-^{2}H$_7$]CA^5-3β-ol	[16,16,17(or20),22,22,23, 23-^{2}H$_7$]CA^4-3-one	555.43	XVII (S-2a)
[16,16,17(or20),22,22,23, 23-^{2}H$_7$] 3β,7α-dihydroxycholest-5-en-27-oic acid	[16,16,17(or20),22,22,23, 23-^{2}H$_7$]CA^5-3β,7α-diol	[16,16,17(or20),22,22,23, 23-^{2}H$_7$]CA^4-7α-ol-3-one	571.42	XVIII (S-2b)
[16,16,17(or20),22,22,23, 23-^{2}H$_7$] 3β,7β-dihydroxycholest-5-en-27-oic acid	[16,16,17(or20),22,22,23, 23-^{2}H$_7$]CA^5-3β,7β-diol	[16,16,17(or20),22,22,23, 23-^{2}H$_7$]CA^4-7β-ol-3-one	571.42	XIX (S-2c)
[16,16,17(or20),22,22,23, 23-^{2}H$_7$] 3β,7α-dihydroxycholest-5-en-27-oic acid methyl ester	[16,16,17(or20),22,22,23, 23-^{2}H$_7$]CA^5-3β,7α-diol-27-methyl ester	[16,16,17(or20),22,22,23, 23-^{2}H$_7$]CA^4-7α-ol-3-one-27-methyl ester	585.44	XX
[16,16,17(or20),22,22,23, 23-^{2}H$_7$] 3β,7β-dihydroxycholest-5-en-27-oic acid methyl ester	[16,16,17(or20),22,22,23, 23-^{2}H$_7$]CA^5-3β,7β-diol-27-methyl ester	[16,16,17(or20),22,22,23, 23-^{2}H$_7$]CA^4-7β-ol-3-one-27-methyl ester	585.44	XXI (S-2d)
3β-hydroxychol-5-en-24-oic acid	BA^5-3β-ol	BA^4-3-one	506.34	XXII (S-3a)
[2,2,4,4,23-^{2}H$_5$] 3β-hydroxychol-5-en-24-oic acid	[2,2,4,4,23-^{2}H$_5$]BA^5-3β-ol	[2,2,4,23-^{2}H$_4$]BA^4-3-one	510.36	XXIII (S-3b)
[2,2,4,4,23-^{2}H$_5$] 3β-hydroxychol-5-en-24-oylglycine	[2,2,4,4,23-^{2}H$_5$]BA^5-3β-ol-24-oylglycine	[2,2,4,23-^{2}H$_4$]BA^4-3-one-24-oylglycine	567.38	XXIV (S-3c)
3β,7α-dihydroxychol-5-en-24-oic acid	BA^5-3β,7α-diol	BA^4-7α-ol-3-one	522.33	XXV (S-3d)
Testosterone[3]	A^4-17β-ol-3-one	A^4-17β-ol-3-one	422.28	XXVI

aqueous methanol (2 mL), the GP hydrazone was eluted from the cartridge with methanol (1 or 2 mL).

The solid-phase extraction step above was modified for the analysis of oxysterols from brain, and the modified procedure was then subsequently used in all further studies. Therefore, for brain samples (and for reference compounds) the GP reaction mixture (3 mL 70% methanol) after overnight incubation was directly applied to a Sep-Pak C$_{18}$ bed (1 cm × 0.8 cm in a glass column) followed by 1 mL of 70% methanol and 1 mL

of 35% methanol. The combined effluent (now 5 mL) was diluted with 4 mL of water. The resulting mixture (now 9 mL in 35% methanol) was again applied to the column followed by a wash with 1 mL of 17% methanol. To the combined effluent 9 mL of water was added. The sample was then in 19 mL of about 17.5% methanol. This was again applied to the column followed by a wash with 10 mL of 10% methanol. Now all the GP derivatives are extracted by the column. They were then eluted with two 1 mL portions of methanol followed by

Table 1. (Continued)

Name	Abbreviation	Oxidation product	Mass of GP	Cmpd (MS/MS Fig[4])
[19,19,19-^{2}H$_3$] testosterone[3]	[19,19,19-^{2}H$_3$]A^4-17β-ol-3-one	[19,19,19-^{2}H$_3$]A^4-17β-ol-3-one	425.30	XXVII

1. mono-GP hydrazone
2. bis-GP hydrazone
3. not treated with cholesterol oxidase
4. MS/MS Figure number, S refers to supplementary material
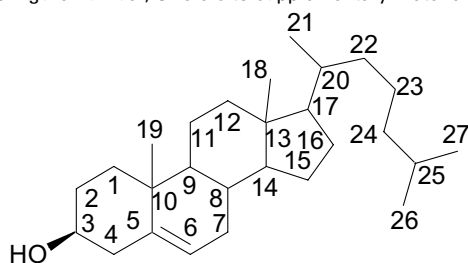
cholesterol skeleton C^5-3β-ol
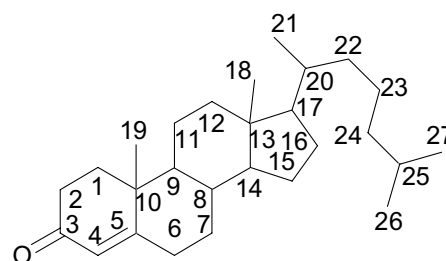
cholest-4-en-3-one skeleton C^4-3-one
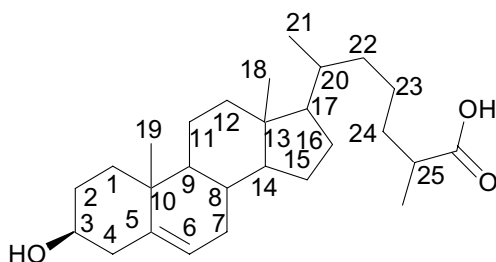
3β-hydroxycholest-5-en-27-oic acid skeleton CA^5-3β-ol
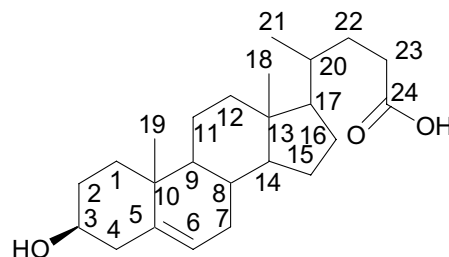
3β-hydroxychol-5-en-24-oic acid skeleton BA^5-3β-ol

1 mL of chloroform/methanol, 1:1 (vol/vol). The three fractions were analyzed separately by ES mass spectrometry. The GP derivatives were found predominantly in the second mL of methanol and the results of the analysis of this fraction are described below.

The derivatization protocol has been applied to mixtures of oxosteroids on the μg-ng level and is suitable for the low level (pg) derivatization of neutral steroids extracted from tissue [36, 37].

Extraction of Oxysterols from Brain

In brief, oxysterols were extracted from 100 mg of rat brain as follows: 100 mg of brain was homogenized in ethanol (1 mL), the ethanol extract was centrifuged and the supernatant retained. The precipitate was ultrasonicated in 1 mL of methanol/dichloromethane (1:1, vol/vol), centrifuged and the supernatant added to that retained previously. The combined supernatants were dried and redissolved in 2 mL of methanol/dichloromethane/water (7:2:1, vol/vol). This solution was added to a Lipidex DEAP (diethylaminohydroxypropyl Sephadex LH-20, PerkinElmer, Beaconsfield, Bucks,

UK) anion-exchange column in its acetate form [50] (7 × 0.4 cm) prepared in methanol/dichloromethane/water (7:2:1, vol/vol). The column was washed with 2 mL of the same solvent, followed by 1 mL of methanol/dichloromethane/water (2:2:1, vol/vol), and the "flow-through" and "wash" combined, dried, and redissolved in 2 mL of hexane/dichloromethane (2:8, vol/vol). This "neutral fraction" was then applied to a Unisil column (8 × 0.8 cm, 200–325 mesh, activated silicic acid, Clarkson Chromatography Products, Inc., South Williamsport, PA) prepared in hexane, and washed with 20 mL of hexane/dichloromethane (2:8, vol/vol) before sample application. Following sample application the column was washed with 80 mL of hexane/dichloromethane (2:8, vol/vol), and eluted with 10 mL of ethylacetate. The eluate was dried and redissolved in 50 μL isopropanol, and used as described above.

Mass Spectrometry

ES mass and collision-induced dissociation (CID) spectra were recorded on Q-TOF Ultima API and Q-TOF Global quadrupole (Q)-orthogonal accelera-

tion (OA) time-of-flight (TOF) instruments, and also on a Quattro Micro tandem quadruple instrument (all Micromass/Waters, Manchester, UK). Each instrument was fitted with a Z-spray nano-ES interface and samples were electrosprayed from metal-coated borosilicate capillaries (Proxeon Biosystems A/S, Odense, Denmark or New Objective, Woburn MA) loaded with 1–5 μL of oxosteroid GP hydrazone (1 ng/μL) in methanol. On the Q-TOF and tandem quadrupole instruments the capillary voltages used were ~1.75 and 1.2 kV, respectively. On the Q-TOF instruments the cone-voltage was 100 V and the RF lens voltage varied between 40 and 200 V. On the tandem quadrupole the cone-voltage was varied between 30 and 60 V, with the RF lens voltage at 0.2 V. With each instrument a counter current of dry nitrogen was used to aid solvent evaporation (cone gas, 40–100 L/h). With the Q-TOF instruments the collision cell located between the quadrupole and TOF sections of the instrument was loaded with argon giving a pressure reading on the near-by "analyzer" Penning gauge of ~ 5×10^{-5} mbar. Gas was maintained in the collision cell when recording both mass and MS/MS spectra. For the recording of mass spectra the potential offset on the collision cell was 10 V (collision energy 10 eV for singly-charged ions). This was varied between 10 and 50 V for the recording of MS/MS spectra. The optimum value was established to be 35 V for singly charged ions, while 17.5 V (35 eV) was used for doubly charged ions. The TOF analyzer could be operated with either "V" (10,000 resolution, full width at half maximum height definition, FWHM) or "W" (17,500 resolution, FWHM) optics. Most spectra were recorded with "W" optics. When MS/MS spectra were recorded on the tandem quadrupole, the hexapole collision cell was loaded with Ar gas so as to give a pressure reading of 3×10^{-3} mbar on the gas-cell Pirani gauge. The collision energy was varied in the range of 10–50 eV. The tandem quadrupole instrument has the additional capacity to record both precursor ion and neutral loss scans.

LC-MS and LC-MS/MS

LC-MS and LC-MS/MS chromatograms were recorded on the Q-TOF Global mass spectrometer interfaced to a Cap-LC low flow-rate chromatography system (Micromass/Waters). Separation was achieved on a C_{18} capillary column (PepMap C_{18} column 180 μm $\times$ 150 mm, 3 μm, 100 A, Dionex, Camberley, Surrey, UK), at a flow-rate set to 1 μL/min. Mobile phase A was 50% methanol, 0.1% formic acid, and mobile phase B consisted of 95% methanol, 0.1% formic acid. Gradient elution was performed starting at 5% B and rising to 60% B over the first 10 min, increasing to 80% B during the next 5 min, and staying at 80% B for a final 10 min, before returning to 5% B.

Results

Oxidation of 3β-Hydroxy-Δ^5 Sterols to 3-Oxo-Δ^4 Sterols

It was found necessary to modify the original procedure of Brooks et al. [47] for the oxidation of 3β-hydroxy-Δ^5 steroids, so as to make it compatible with the ES-MS analysis of oxosterols and their GP hydrazones. Isopropanol is a good solvent for oxysterols, and cholesterol oxidase was found to be still active when a solution of oxysterol(s) in 50 μL of isopropanol was added to 1 mL of the enzyme in 50 mM phosphate buffer at pH 7. The use of detergent to solubilize the enzyme and the oxysterols was avoided, as it was found be difficult to completely remove the detergent from the oxidation products. After a suitable incubation period, our normal procedure was then to add methanol, GP hydrazine and glacial acetic acid so as to obtain the derivative directly without isolation of the ketone intermediate. In preliminary experiments, however, the efficiency of the oxidation reaction was evaluated by analysis of the ketone formed before derivatization. This was achieved by terminating the oxidation reaction by addition of methanol to the reaction solution and extracting the oxosterols on a C_{18} column using a recycling method. By using the "recycling" method of solid-phase extraction it was possible to apply the oxosterols to the C_{18} column in a solution of high methanol content (50% methanol). This was desirable to ensure that the oxosterols were dissolved-in, rather than dispersed-in, solution. The initial flow-through from the C_{18} column was collected and diluted with water so as to decrease its elutropic strength, the diluted flow-through was then recycled through the column. Any oxosterols not retained by the column following their initial application were subsequently extracted by the column on reapplication of the diluted flow-through. To monitor the efficiency of the purification of oxosterols the entire procedure was carried out using ^{14}C-labeled cholesterol. Radioactivity was found to be exclusively retained on the column, and then completely eluted with methanol.

The activity of the enzyme under the solution conditions employed for the oxidation reaction was evaluated with the use of 3β-hydroxycholest-5-en-27-oic and 3β-hydroxychol-5-en-24-oic acids. Both of these acids will give [M − H]$^-$ ions upon negative-ion ES ionization, and hence their oxidation reactions can be monitored by the decrease in [M − H]$^-$ ion currents and the complementary increase in ion current of the oxidation products. Under the reaction conditions employed the oxidation reactions were found to proceed to completion.

The choice of reaction time may have to be determined by the exact aim of the analysis. Compounds having additional substituents in the A-ring and steroids with no (C_{19}) or a short (C_{21}) side-chain react much slower than cholesterol (see reference [48] for a

table of reaction rates for different steroids). We investigated the effect of an extended reaction time on the oxidation of cholesterol and found that minor products with additional oxygens were formed when the oxidation time exceeded 5 h, indicating that the cholest-4-en-3-one underwent further oxidation.

Although not the focus of the current study, 5α-steroids with a 3β-hydroxy group can be oxidized to 3-oxo-5α-steroids. Using the above procedure lathosterol (3β-hydroxy-5α-cholest-7-ene, 5α-C^7-3β-ol) was successfully oxidized to its 3-oxo equivalent (5α-C^7-3-one), as were a number of other 3β-hydroxy-5α-steroids.

Derivatization of Oxosterols

The derivatization of oxosterols to GP hydrazones was carried out essentially as described previously [38, 39]. However, it was found to be necessary to modify the reaction conditions for the derivatization of oxosterols with a labile 7-hydroxy-Δ^4-3-oxo structure which otherwise underwent partial elimination of water with formation of a dienone. This was achieved by allowing the reaction to proceed at room temperature over night. Under these milder conditions, the efficiency of the derivatization reaction was monitored using 3-oxocholest-4-en-27-oic (CA^4-3-one) and 3-oxochol-4-en-24-oic (BA^4-3-one) acids, which in their underivatized forms give [M − H]$^-$ ion signals in ES spectra. After 12 h, the signals for the underivatized acids were found to fall to zero. It should be noted that for the majority of studies, the derivatization reaction was carried out directly on the products of the cholesterol oxidase reaction, without any further purification or extraction.

Oxosteroids with structures other than 3-oxo-Δ^4 were successfully derivatized with the GP reagent. For example, 5α-cholestan-3-one (5α-C-3-one), 17α-acetoxy-5α-androstan-3-one (5α-A-17α-acetoxy-3-one), $20\beta,21$-dihydroxy-5β-pregnan-3-one (5β-P-$20\beta,21$-diol-3-one) were converted to their 3-GP hydrazones; while 3β-hydroxy-5α-cholestan-7-one (5α-C-3β-ol-7-one), 7-oxocholesterol (C^5-3β-ol-7-one), 3β-hydroxy-5α-cholest-8(14)-en-15-one (5α-C$^{8(14)}$-3β-ol-15-one), a kind gift from G. Schroepfer, and $3\beta,17\beta$-dihydroxy-androst-5-en-16-one (A^5-$3\beta,17\beta$-16-one) were converted to 7-GP, 7-GP-Δ^5, 15-GP-D$^{8(14)}$, and 16-GP-Δ^5 hydrazones, respectively. Additionally, cholesta-4,6-dien-3-one (C^{4,6}-3-one) was successfully converted to a 3-GP hydrazone, and the plant sterol campesterol (C^5-24α-methyl-3β-ol) was successfully oxidized and derivatized to a 3-oxo-Δ^4-3-GP hydrazone. Steroids containing two oxo groups were converted to mono- and to a minor extent to bis-GP derivatives. Depending on the position of the second oxo group (i.e., the one not at C-3), the formation of the bis-GP derivative was sometimes more pronounced (e.g., 3,17-, 3,6- and 3,22-diones). Further studies are required to establish the reaction rates for steroids with multiple oxo groups.

Tandem Mass Spectrometry of Oxosterol GP Hydrazones

Instrumental effects. Three tandem mass spectrometers were used in this study each fitted with a nano-ES source. Two of the instruments were of Q-TOF type, the third was a tandem quadrupole. At a defined collision energy, the three instruments gave similar but not identical spectra. Some instrumental effects were noted, in particular the transmission of low-mass fragments-ions (<200 Da) was found to be greater on the tandem quadrupole than on the Q-TOF instruments. This is illustrated in Figure 1, which shows 35 eV CID spectra of C^4-24-ol-3-one GP hydrazone (**VI**) recorded on the tandem quadrupole (1a), Q-TOF Ultima API (1b), and Q-TOF Global (1c) instruments. Note that in the spectrum recorded on the Q-TOF instruments (Figure 1b and c) the m/z ranges 50–121 and 122–390 have been magnified. The Q-TOF instruments also provide much higher product-ion resolution than the tandem quadrupole instrument. Using the Q-TOF instruments and employing "W" ion-optics, the product-ion resolution was of the order of 17,500 (FWHM), this in combination with the excellent stability of the instruments' m/z range allowed the routine acquisition of accurate mass data (±5–10 ppm).

In MS/MS spectra, 3-oxo-Δ^4 sterol GP hydrazones give four main types of fragment ion: (i) those derived from the GP hydrazone group, (ii) those resulting from steroid ring and C-17 side-chain fragmentation and which contain the hydrazone group, (iii) those which are a result of the neutral loss of pyridine, carbon monoxide and water from the molecular ion, and (iv) those which correspond to small hydrocarbon ions (Schemes 2 and 5). Conveniently, ions in groups (i)–(iii) predominantly fall within distinct m/z ranges, i.e., (i) 50–121; (iia) 121–180; (iib) 180–390; and (iii) above 390, and despite differences in absolute ion transmission between the instruments, within defined m/z ranges the instruments give normalized MS/MS spectra which are quite similar, and allow a number of generalizations to be made concerning the low-energy CID of oxosterol GP hydrazones.

Group (i) fragment ions: GP hydrazone fragment ions. In all of the MS/MS spectra of the 3-oxo-Δ^4 sterols studied a series of fragment ions characteristic of the GP hydrazone group is observed at m/z 80.05, 94.07, 109.08, 120.05 and 137.07. High-resolution accurate mass data shows that these ions have the compositions C_5H_6N (σ_1 + H), $C_5H_5NCH_3$ (σ_2 + H), $C_5H_5NCH_2NH_2$ (σ_4 + H-CO), C_5H_5NCHCO (σ_3 − H), and $C_5H_5NCH_2CONH_2$ (σ_4 + H), respectively (Scheme **2**). The peaks at 109 and 120 are in fact doublets consisting of $C_5H_5NCH_2NH_2/C_8H_{13}$ (109.08/109.10) and $C_5H_5NCHCO/C_8H_{10}N$ (120.05/120.08), respectively, which are easily resolved on the Q-TOF instrument operated in the "W"-mode. The fragment-ion at m/z 80.05, abundant in the CID spectra re-
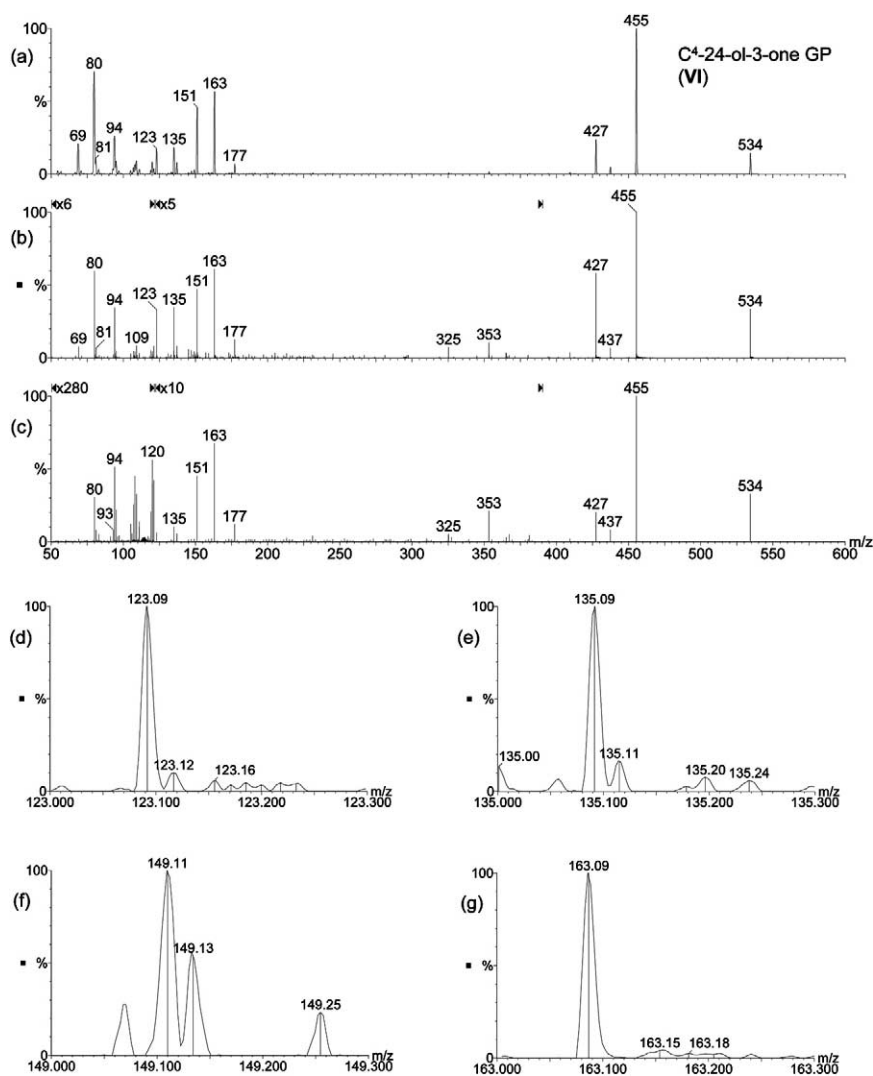
Figure 1. MS/MS spectra of the $[M]^+$ ion of C^4-24-ol-3-one GP hydrazone (**VI**, m/z 534). Spectra recorded on (**a**) tandem quadruple; (**b**) Q-TOF Ultima API, "W-mode"; (**c**) Q-TOF Global, "W-mode". Collision energy 35 eV. Expanded views of the peaks at m/z 123 (**d**); 135 (**e**), 149 (**f**), and 163 (**g**) from spectrum (**c**). In the spectra presented in (**a**), (**b**), and (**c**) the ratio of fragment ions 123.09:135.09:149.11 are 9:10:2, 9:10:1 and 6:10:2, respectively. In (**b**) and (**c**), regions m/z 50–121 and 122–390 have been magnified by factors of 6 and 5, and 280 and 10, respectively. The y-axis represents relative abundance. 1–5 μL of sample (1 ng/μL) was loaded into the nano-ES capillary, and about 1 μL consumed for the acquisition.

corded on the tandem quadrupole instrument, is an ideal target ion for precursor-ion scanning.

3-Oxo-Δ^4 Sterols: Compounds V–XVI (see Table 1)

Group (iia) fragment ions: Steroid skeleton fragment ions. 3-Oxo-Δ^4 sterol GP hydrazones undergo fragmentation in the steroid-ring in an identical fashion to other 3-oxo-Δ^4 steroid GP hydrazones [38]. In the absence of additional substituents on the ABC rings, 3-oxo-Δ^4 steroid GP hydrazones give two major series of fragment ions at m/z 151.09 ($^*b_1$-12), 163.09 ($^*b_2$-CH_2/ $^*b_3$-C_2H_4) and 177.10 ($^*b_2$); and at 123.09 ($^\#b_1$-12), 135.09 ($^\#b_2$-CH_2/$^\#b_3$-C_2H_4) and 149.11 ($^\#b_2$) (Figures 1 and 2) [38, 39]. The $^*b$ ion-series corresponds to B-ring frag-

ment ions which have additionally lost the pyridine ring of the GP hydrazone group, while the $^\#b$ ion-series corresponds to B-ring fragments where the pyridine ring and CO groups have been lost (Scheme 2) [38, 39]. Griffiths et al. have shown that the $^*b_1$-12, $^*b_2$-CH_2/$^*b_3$-C_2H_4 and $^*b_2$ ions are formed via a $[M-79]^+$ intermediate (which corresponds to the molecular-ion having lost the pyridine ring), while the $^\#b_1$-12, $^\#b_2$-CH_2/$^\#b_3$-C_2H_4 and $^\#b_2$ ions are formed via a $[M-79-28]^+$ intermediate (Scheme 2) [38, 39]. Detailed studies using heavy-isotope labels have shown the $^*b_1$-12 and $^\#b_1$-12 ions to contain the A-ring plus C-19, but minus C-5; and the $^*b_2$ and $^\#b_2$ ions to contain the A-ring plus C-19 and C-6 (Scheme 3) [38, 39]. The hypothesized $^*b_2$-CH_2 and $^\#b_2$-CH_2 fragments may more accurately be described as
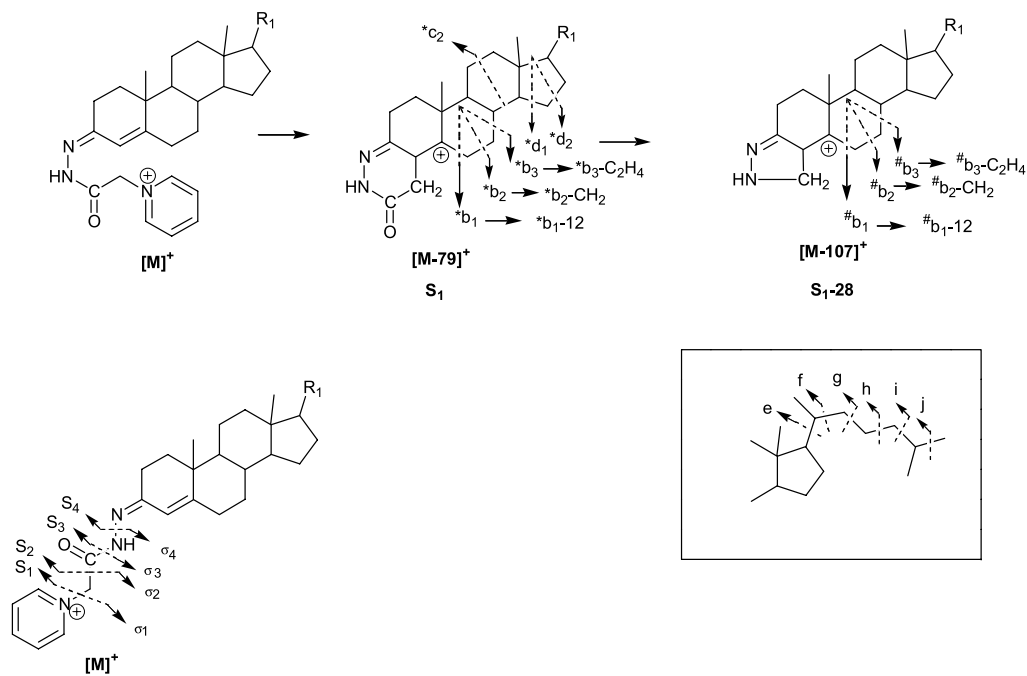
Scheme 2.   Fragmentation pattern of 3-oxo-Δ^4 steroid 3-GP hydrazones.

$*b_2$-CH$_3$-H+2H and $^\#b_2$-CH$_3$-H+2H ions. These ions are suggested to contain the A-ring and C-6, but C-19 has been lost and replaced by an H-atom from C-7 or the CD-rings, additionally the β-H on C-6 has been replaced by an H-atom from C-7 or the CD-rings [49]. The $*b_3$-C$_2$H$_4$ and $^\#b_3$-C$_2$H$_4$ ions contain the A-ring plus C-6 and C-7, but C-19 and C-10 have been lost as has a H-atom, probably the β-H from C-6 [52]. In 3-oxo-Δ^4 GP hydrazones containing no further A or B ring substituents the $*b_3$-C$_2$H$_4$ and $*b_2$-CH$_3$-H+2H ions have identical elemental formula, as have the $^\#b_3$-C$_2$H$_4$ and $^\#b_2$-CH$_3$-H+2H ions [53]. Supporting evidence for the structures of the B-ring fragment ions described above (Scheme **3**) has been obtained in the current study where the $*b_1$-12 and $^\#b_1$-12; $*b_2$-CH$_2$/$^\#b_3$-C$_2$H$_4$ and $^\#b_2$-CH$_2$/$^\#b_3$-C$_2$H$_4$; and $*b_2$ and $^\#b_2$ fragment-ions from [2,2,4,23-^{2}H$_4$]BA^4-3-one and [2,2,4,23-^{2}H$_4$]BA^4-3-one-24-oylglycine GP hydrazones (**XXIII** and **XXIV** respectively) were each found to be +3 Da heavier than the equivalent ions from the monoisotopomers see Figure S-3 in the Supplementary Material section (which can be found in the electronic version of this article.). It should be noted that the peaks at m/z 123, 135, 149, and 163 consisted of doublets (Figure 1d–g). This is evident when spectra are recorded at high-resolution with the Q-TOF instruments operated with "W" ion-optics. At m/z 123.12, 135.12, 149.13, and 163.15 peaks corresponding to C$_9$H$_{15}$, C$_{10}$H$_{15}$, C$_{11}$H$_{17}$ and C$_{12}$H$_{19}$ respectively, are resolved from those at 123.09 ($^\#b_1$-12, C$_7$H$_{11}$N$_2$), 135.09 ($^\#b_2$-CH$_2$/$^\#b_3$-C$_2$H$_4$, C$_8$H$_{11}$N$_2$), 149.11 ($^\#b_2$, C$_9$H$_{13}$N$_2$), and 163.09 ($*b_2$-CH$_2$/$*b_3$-C$_2$H$_4$, C$_9$H$_{11}$N$_2$O).

Addition of a 7-hydroxy group to the steroid skeleton drastically alters the pattern of B-ring fragment ions for 3-oxo-Δ^4 sterol GP hydrazones (Figure 2). Fragment ions at m/z 135, 149, 163, and 177 are attenuated in the spectra of 7-hydroxy-3-oxo-Δ^4 steroid GP hydrazones, and accurate mass measurements at high-resolution confirm that it is the $^\#b_2$-CH$_2$, $^\#b_2$, $*b_2$-CH$_2$, and $*b_2$ components at these integer masses which are reduced in abundance. In the spectrum of a 7-hydroxy-3-oxo-Δ^4 steroid GP hydrazone the $^\#b_3$-C$_2$H$_4$, and $*b_3$-C$_2$H$_4$ fragment ions are expected to be shifted to m/z 151.09 (135.09 + 15.99, C$_8$H$_{11}$N$_2$O) and 179.08 (163.09 + 15.99, C$_9$H$_{11}$N$_2$O$_2$), respectively. Significantly, in the CID spectrum of C^4-7β-ol-3-one GP hydrazone (**V**) (Figure 2e) the abundance of ions at m/z 151.09 and 179.08, corresponding to ions of composition C$_8$H$_{11}$N$_2$O and C$_9$H$_{11}$N$_2$O$_2$, are enhanced in comparison to CID spectra of C^4-24-ol-3-one (**VI**) (Figure 2a and b), C^4-25-ol-3-one (**VII**) (Figure 2c), and C^4-27-ol-3-one (**VIII**) (Figure 2d). The elemental composition C$_8$H$_{11}$N$_2$O (m/z 151.09) corresponds to a $*b_1$-12 ion, a $^\#b_3$-C$_2$H$_4$ ion and also a $^\#b_2$-CH$_3$-H + H + OH ion in C^4-7β-ol-3-one GP hydrazone (**V**). The elemental composition C$_9$H$_{11}$N$_2$O$_2$ (m/z 179.08) corresponds to a $*b_3$-C$_2$H$_4$ ion or a $*b_2$-CH$_3$-H + H + OH. It is not surprising that the intensity of the peaks corresponding to $^\#b_2$ (m/z 149.11) and $*b_2$ (m/z 177.10) are attenuated in the CID spectra of 7-hydroxy-3-oxo-Δ^4 steroid GP hydrazones, as dehydration in the B-ring would lead to the introduction of a double-bond between C-6 and C-7 and resonance stabilization of the positive-charge (Scheme 4). With the blocking of the $^\#b_2$ and $*b_2$ fragmentation channels, additional ion current could then be channelled through to the $^\#b_1$-12 (m/z 123.09) and $*b_1$-12 (m/z 151.09) fragments.

In the CID spectra of 7-hydroxy-3-oxo-Δ^4 steroid GP hydrazones (e.g., Figure 2e) the fragment ion at m/z 179.08 corresponds to $*b_2$-CH$_3$-H + H + OH and to

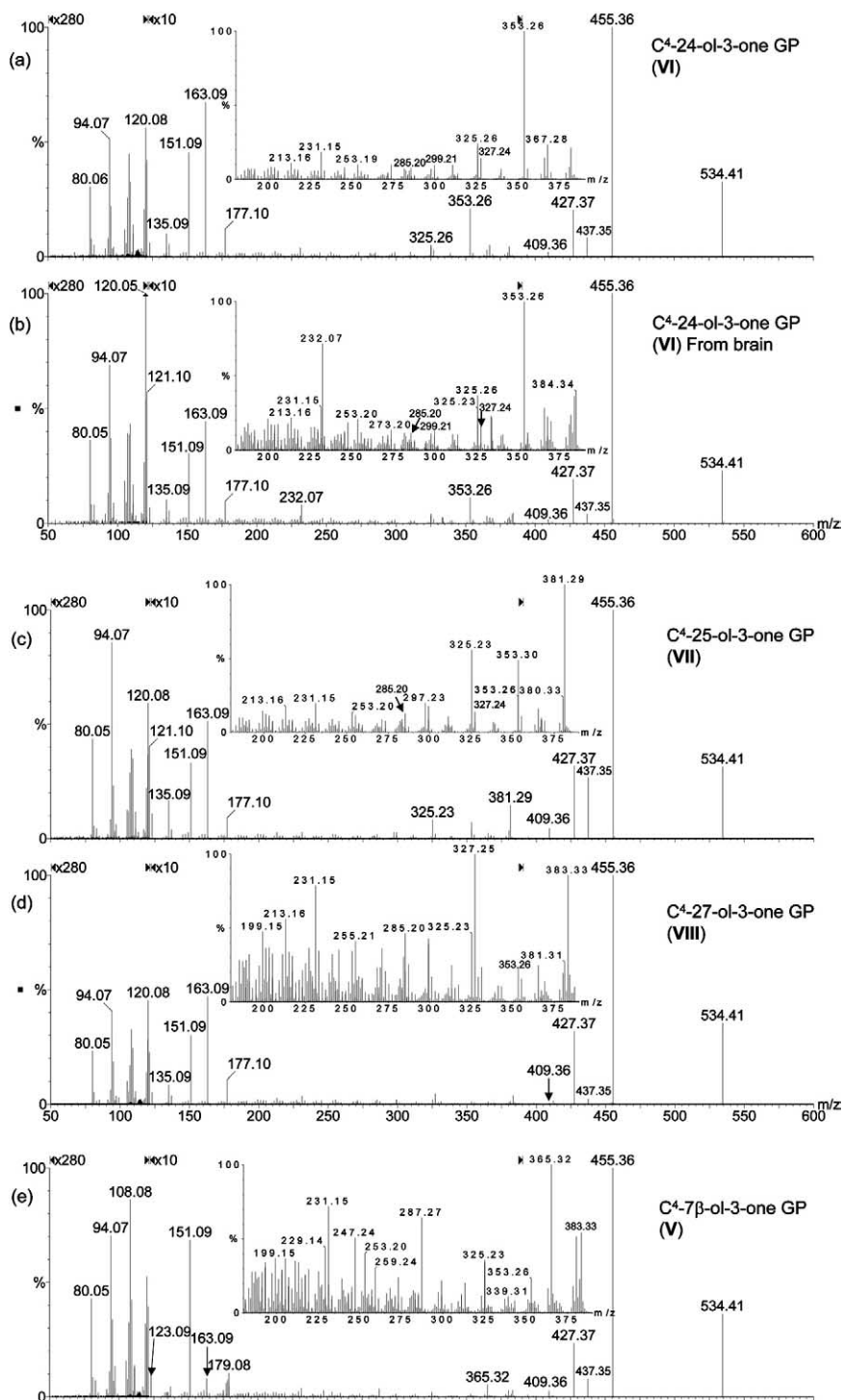**Figure 2.** MS/MS spectra of the [M]$^+$ ion of GP hydrazones (**a**) C^4-24-ol-3-one (**VI**, *m/z* 534.41); (**b**) C^4-24-ol-3-one from brain (**VI**, *m/z* 534.41); (**c**) C^4-25-ol-3-one (**VII**, *m/z* 534.41); (**d**) C^4-27-ol-3-one (**VIII** *m/z* 534.41); (**e**) C^4-7β-ol-3-one (**V**, *m/z* 534.41); (**f**) C^4-3,22-dione (**X**, *m/z* 532.39). The spectra in (**a**)–(**f**) are of 3-GP hydrazones, that in (**g**) is of the [M]$^{2+}$ ion of C^4-3,22-dione 3,22-bisGP hydrazone (**XI**, *m/z* 333.23). (**h**) Expanded views of the peaks at *m/z* 325 and 353 recorded at 17,500 (top panel) or 12,000 (central and bottom panel) resolution, FWHM definition. The upper panels in (**h**) show peaks from C^4-24-ol-3-one GP (**VI**); the central panels in (**h**) show peaks from C^4-25-ol-3-one GP (**VII**); and the bottom panels in (**h**) show peaks from C^4-27-ol-3-one GP (**VIII**). In the spectra presented in (**a**)–(**g**) the ratio of fragment ions 123.09:135.09:149.11 and 151.09:163.09:177.10 are 6:10:2 and 7:10:2 (**a**); 7:10:2 and 7:10:2 (**b**); 7:10:2 and 6:10:2 (**c**); 6:10:2 and 6:10:2 (**d**); 10:2:1 and 10:1:1 (**e**); 7:10:1 and 8:10:1 (**f**); 6:10:2 and
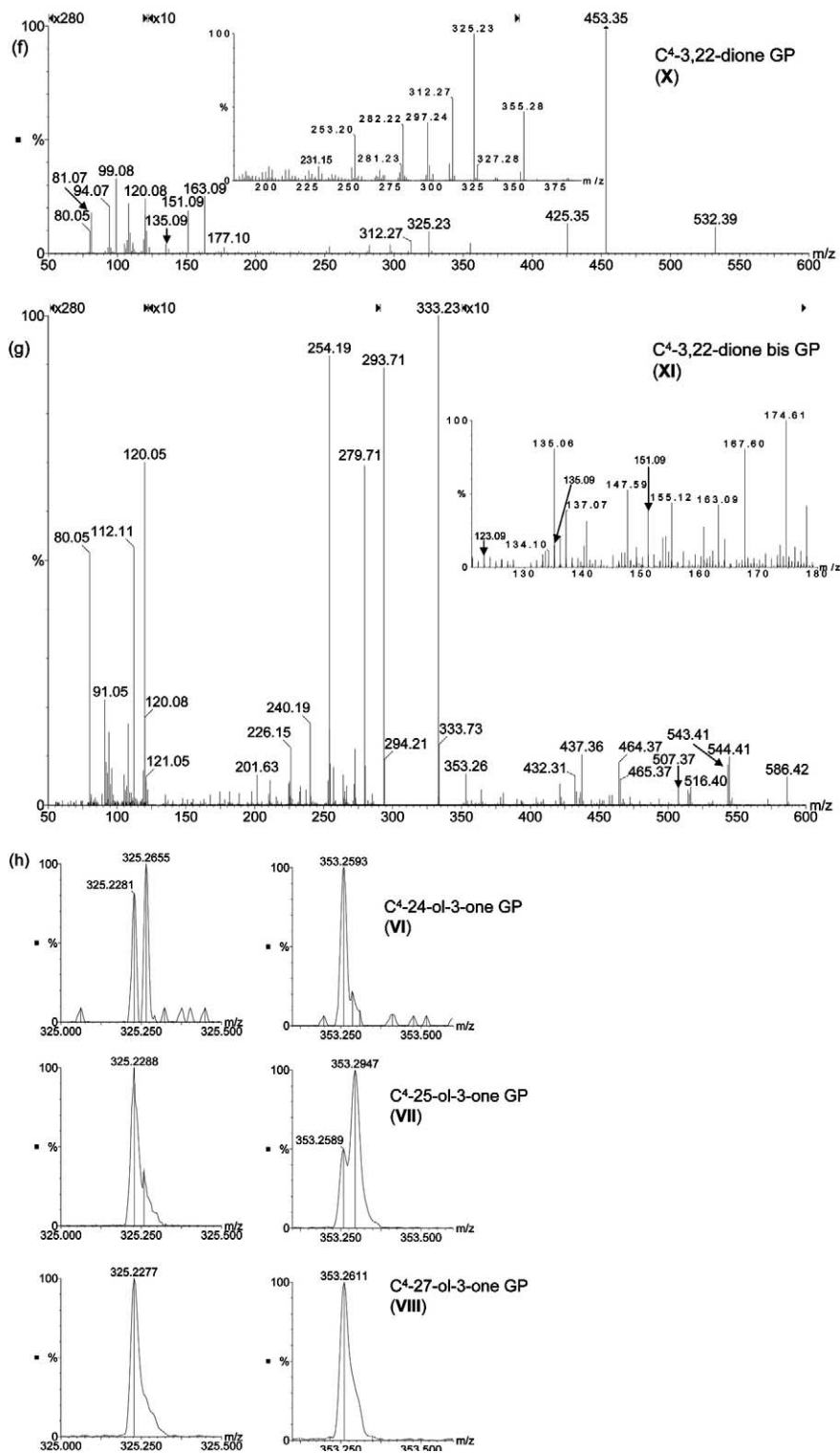
Figure 2 (continued). 10:10:2 (**g**). In (**a**)–(**f**) the *m/z* regions 50–121 and 122–390 have been magnified by a factor of 280 and 10, respectively. In (**g**) the regions 50–121, 122–290, and 350–600 have been magnified by a factor of 280, 10, and 10, respectively. The y-axis represents relative abundance. All spectra recorded on the Q-TOF Global instrument in "W-mode" at a collision energy 35 eV. 1–5 μL of sample [1 ng/μL for steroid standards and 10 μg brain/μL in (**b**)] was loaded into the nano-ES capillary, and about 1 μL consumed for the acquisition.
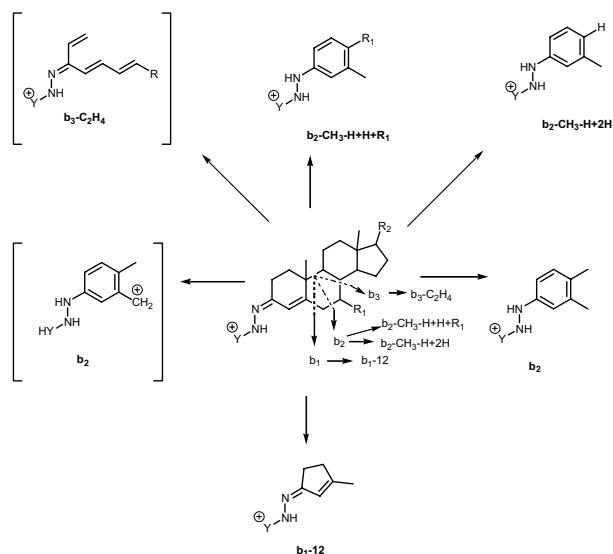
Scheme 3. Structures of b-type fragment ions. For simplicity the hydrazone has been drawn as a linear chain; alternatively the Y-group can be bound to C-4 with charge located on the A-ring. In *b-type ions Y = COCH$_2$, in #b-type ions Y = CH$_2$. The structures in brackets are analogous to those suggested to correspond to fragment ions of protonated testosterone [52].

*b$_3$-C$_2$H$_4$ ions. The *b$_2$-CH$_3$-H + H + OH ion is analogous to the *b$_2$-CH$_3$-H + 2H ion normally observed at m/z 163.09 (Figure 2a–d), but where an OH-group rather than H-atom is transferred from C-7 to the ion (Scheme 3). The #b$_2$-CH$_3$-H + H + OH and #b$_3$-C$_2$H$_4$ ions have an identical elemental composition to a *b$_1$-12 ion and also contribute to the enhanced intensity of the ion at m/z 151.09. This was evident when CID spectra were recorded of [M-107]$^+$ ions from 7-hydroxy-3-oxo-Δ^4 steroid GP hydrazones which can not fragment to give *b-12 ions, but were observed to give abundant fragment ions at m/z 151.09 corresponding to #b$_2$-CH$_3$-H +H + OH and #b$_3$-C$_2$H$_4$ ions (data not shown).

Group (iib) fragment ions: Minor (low abundance) ring and C-17 side-chain fragment ions. While the major cleavages in the steroid ring system occur in the B-ring and give abundant fragment ions, minor but important fragment ions are generated by cleavages in the C- and D-rings and in the C-17 side-chain giving ions of lower abundance. In the CID spectra of 3-oxo-Δ^4 sterol GP hydrazones *c$_2$, *d$_1$, *d$_2$ *e-H, and/or *e + H fragment ions are consistently observed at m/z 231.15 (C$_{14}$H$_{19}$N$_2$O), 285.20 (C$_{18}$H$_{25}$N$_2$O), 299.21 (C$_{19}$H$_{27}$N$_2$O), 325.23 (C$_{21}$H$_{29}$N$_2$O), and/or 327.24 (C$_{21}$H$_{31}$N$_2$O) (e.g., cmpds **VI-VIII**, Figure 2a–d, Scheme **2**). Incorporation of a C-24 hydroxyl group results in the additional appearance of #f-H and *f-H fragment ions at m/z 325.26 (C$_{22}$H$_{33}$N$_2$) and 353.26 (C$_{23}$H$_{33}$N$_2$O) (**VI**), (Figure 2a and b). These fragment ions are absent or much weaker in the spectra of C^4-25-ol-3-one (**VII**) and C^4-27-ol-3-one (**VIII**) (Figure 2c, d, and h). The presence of the 25-hydroxyl group in C^4-25-ol-3-one (**VII**) facilitates frag-

mentation between C-23 and C-24 with the formation of comparatively abundant fragment ions at 353.30 (#h-H, C$_{24}$H$_{37}$N$_2$) and 381.29 (*h-H, C$_{25}$H$_{37}$N$_2$O) (Figure 2c). Incorporation of two hydroxyl groups in the C-17 side-chain as in C^4-20R,22R-diol-3-one GP hydrazone (**XII**) results in enhanced abundance of fragment ions at 299.25 (C$_{20}$H$_{31}$N$_2$), 327.24 (C$_{21}$H$_{31}$N$_2$O), and 353.26 (C$_{23}$H$_{33}$N$_2$O) corresponding to #e+H, *e+H and *f+H-H$_2$O respectively (Figure 3b). Altering the steroid ring system by introduction of a labile 7-hydroxy group results in the formation of *c$_2$-H$_2$O, *c$_2$ + 2H-H$_2$O, *e-H-H$_2$O, and/or *e + H-H$_2$O fragment ions at m/z 229.13 (C$_{14}$H$_{17}$N$_2$O), 231.15 (C$_{14}$H$_{19}$N$_2$O), 323.21 (C$_{21}$H$_{27}$N$_2$O), and/or 325.23 (C$_{21}$H$_{29}$N$_2$O), respectively, (Scheme **4**, Figure 2e, Figure 3a, and Supplementary Material Figure S-1). The combined presence of 7- and 25-hydroxyl groups on the C^4-3-one template (**XIII, XIV**) results in enhanced intensity of a fragment ion at 341.22 (C$_{21}$H$_{29}$N$_2$O$_2$) corresponding to *e-H, particularly in spectra of the 7β isomer (**XIV**). In contrast, the 7α isomer shows enhanced abundance of an ion at 203.15 (#c$_2$ + 2H-H$_2$O, C$_{13}$H$_{19}$N$_2$) and at 231.15 (*c$_2$ + 2H-H$_2$O, C$_{14}$H$_{19}$N$_2$O) (**XIII**). Similarly, in spectra of C^4-7α,27-diol-3-one (**XV**), the fragment ions at 203.15 and 231.15 are comparatively abundant, but fragment ions are not observed at 341.22.

Group (iii) fragment ions: GP hydrazone neutral-loss fragment ions. Each of the 3-oxo-Δ^4 sterol GP hydrazones investigated in the present study give [M-79]$^+$ and [M-107]$^+$ fragment ions which are formed by the neutral-loss of pyridine; and pyridine plus CO, respectively (Scheme **2**). Similar fragment ions were observed in the MS/MS spectra of other 3-oxo-Δ^4 steroid GP hydrazones [38, 39]. The added presence of hydroxyl groups on the cholest-4-en-3-one skeleton results in the additional formation of [M-79-(n18)]$^+$ and [M-107-(n18)]$^+$ ions, where n is the number of additional hydroxyl groups. The relative intensities of these ions depend on the location of the hydroxyl groups. From the MS/MS
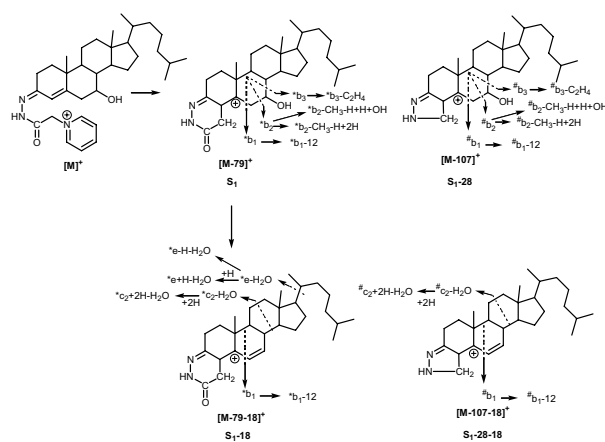
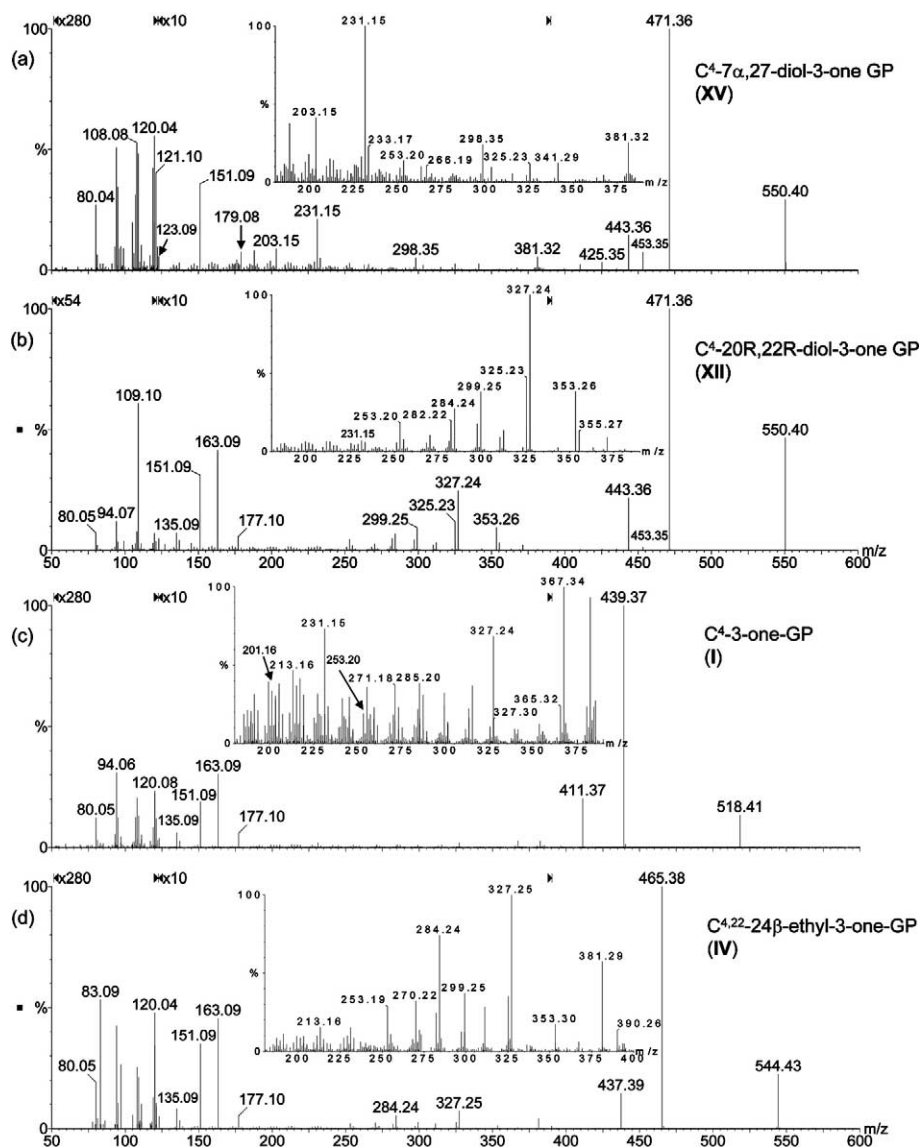**Scheme 4.** Fragmentation pattern of 7-hydroxy-3-oxo-Δ^4 steroid GP hydrazone.

Figure 3. MS/MS spectra of the $[M]^+$ ion of GP hydrazones of (**a**) C^4-7α,27-diol-3-one (**XV**, m/z 550.40); (**b**) C^4-20R,22R-diol-3-one (**XII**, 550.40); (**c**) C^4-3-one (**I**, m/z 518.41); (**d**) $C^{4,22}$-24β-ethyl-3-one (**IV**, m/z 544.43). In the MS/MS spectra the ratio of fragment ions 123.09:135.09:149.11 and 151.09:163.09:177.10 are 10:1:1 and 10:1:1 (**a**); 7:10:1 and 8:10:1 (**b**); 6:10:2 and 6:10:2 (**c**); 6:10:1 and 8:10:1 (**d**). In (**a**), (**c**), and (**d**) the m/z regions 50–121 and 122–390 have been magnified by a factor of 280 and 10, respectively, while in (**b**) by a factor of 54 and 10, respectively. The y-axis represents relative abundance. All spectra recorded on the Q-TOF Global instrument in "W-mode" at a collision energy 35 eV. 1–5 μL of sample (1 ng/μL) was loaded into the nano-ES capillary, and about 1 μL consumed for the acquisition.

spectra recorded of monohydroxy-3-oxo-Δ^4 steroid GP hydrazones, the order of hydroxyl-group lability giving $[M-79-18]^+$ and $[M-107-18]^+$ ions at 437.35 and 409.36 was determined to be 25-OH >24-OH $\sim$ 7 -OH >27-OH (Figure 2). This difference in the ease of dehydration between sterol isomers aids in their differentiation when not present in a mixture.

The hydroxyl groups at 20R and 22R are surprisingly stable, and in the CID spectrum of C^4-20R,22R-diol-3-one GP hydrazone (**XII**) the $[M-79-(n18)]^+$ at 453.35 and 435.34; and $[M-107-(n18)]^+$ ions at 425.35 and 407.34 are present at less than 2% of the intensity of the $[M-79]^+$

ion (Figure 3b). In contrast, the hydroxyl group on C-25 is labile, this is evident in the CID spectra of C^4-7β,25-diol-3-one (**XIV**) and C^4-7α,25-diol-3-one (**XIII**) GP hydrazones (see Supplementary Material Figure S-1), where strong/medium intensity $[M-79-18]^+$ fragment ions are observed at m/z 453.35 (RA 55%, 20%), as are weaker satellite peaks corresponding to $[M-79-(2 \times 18)]^+$ at m/z 435.34 (RA 5%, 5%), and $[M-107-18]^+$ at m/z 425.35 (RA 5%, 5%). Peaks are also observed at m/z 407.34 from the C^4-7,25-diol-3-one isomers, corresponding to fragments $[M-107-(2 \times 18)]^+$, but these are of low intensity (RA 2%, 2%). In comparison, when the side-

chain hydroxyl group is shifted from C-25 to C-27 as in C^4-7α,27-diol-3-one GP hydrazone (**XV**), [M-79-18]$^+$ and [M-107-18]$^+$ ions are observed to give comparatively weak peaks (m/z 453.35, 5%; m/z 425.35, RA) (Figure 3a).

Bile Acids, Compounds XVII–XXV: And 22-Oxocholesterols, Compounds X–XI (see Table 1)

Cholest-5-en-27-oic acids are intermediates in the conversion of cholesterol to bile acids, and 3β-hydroxycholest-5-en-27-oic acid and its 7α-hydroxylated product 3β,7α-dihydroxycholest-5-en-27-oic acid are quantitatively dominating unconjugated bile acids in the human circulation [1, 3]. After oxidation of these compounds with cholesterol oxidase and derivatization with GP hydrazine, the resulting 3-oxo-Δ^4 acids undergo CID reactions to give fragment ions in accord with their structural features as discussed above (see Supplementary Material Figure S-2). For example, CID of [16,16,17(or 20),22,22,23,23-$^2H_7$]CA^4-3-one GP hydrazone (**XVII**) gives the $^\#b$-type fragment ions $^\#b_1$-12 (m/z 123.09), $^\#b_2$-CH_2/$^\#b_3$-C_2H_4 (m/z 135.09) and $^\#b_2$ (m/z 149.11); and the $^*b$-type fragment ions $^*b_1$-12 (m/z 151.09), $^*b_2$-CH_2/$^*b_3$-C_2H_4 (m/z 163.09) and $^*b_2$ (m/z 177.10): while in CID spectra of 7-hydroxylated acids (and methyl esters), B-ring fragment ion peaks $^\#b_2$-CH_2 (m/z 135.09), $^\#b_2$ (m/z 149.11), $^*b_2$-CH_2 (m/z 163.09) and $^*b_2$ (m/z 177.10) are attenuated. The presence of a 7-hydroxy group on the steroid skeleton results in enhanced intensity of the peak at m/z 151.09 corresponding to $^\#b_3$-C_2H_4 and $^*b_1$-12, and also m/z 179.08 corresponding to $^*b_3$-C_2H_4.

Ions of minor abundance but of structural importance are generated by cleavages in the C- and D-rings and the C-17 side-chain. In the CID spectrum of [16,16,17(or 20),22,22,23,23-$^2H_7$]CA^4-3-one GP hydrazone (**XVII**) fragment ions characteristic of 3-oxo-Δ^4 sterols are observed at m/z 231.15, 285.20, 299.21 corresponding to $^*c_2$, $^*d_1$, and $^*d_2$ cleavages. A cluster of ions from 327.24 ($C_{21}H_{27}D_2N_2O$, [$^2H_2$]*e-H) to 330.26 ($C_{21}H_{28}D_3N_2O$, [$^2H_3$]*e + H) is also seen corresponding to *e-H and *e + H fragment ion with differing degrees of deuteration. As was the case with the oxosterols discussed above, altering the steroid ring system by introduction of a labile 7-hydroxy group results in the formation of $^*c_2$-H_2O, and $^*c_2$ + 2H-H_2O, fragment ions at m/z 229.13, and 231.15; and a cluster of ions corresponding to *e-H-H_2O and *e + H-H_2O between 325.22 ($C_{21}H_{25}D_2N_2O$, [$^2H_2$]*e-H-H_2O) and 328.25 ($C_{21}H_{26}D_3N_2O$, [$^2H_3$]*e + H-H_2O). As in the spectrum of C^4-7α,27-diol-3-one fragment ions are also observed at 203.15 ($^\#c_2$ + 2H-H_2O).

As in the spectra of oxysterol GP hydrazones, [M-79-18]$^+$ and [M-107-18]$^+$ ions are observed in the spectra of the 27-oic acids. The presence of these ions at m/z 458.38 (RA 2%) and 430.38 (RA 2%) in the spectrum of [16,16,17(or 20),22,22,23,23-$^2H_7$]CA^4-3-one (**XVII**) shows that water can be eliminated from the C-27 acid group. In the spectra of the 7-hydroxy acids the intensity of the [M-79-18]$^+$ and [M-107-18]$^+$ ions at 474.37 (RA 5%) and 446.38 (RA 5%) are enhanced, and additional minor intensity peaks at 456.36 (RA <2%) and 428.37 (RA 2%) corresponding to [M-79-(2 × 18)]$^+$ and [M-107-(2 × 18)]$^+$ are observed. Predictably, the spectra of the 24-methyl esters of the [16,16,17(or 20),22,22,23,23-$^2H_7$]CA^4-7-ol-3-one GP hydrazones (**XX and XXI**) show [M-79-18]$^+$, [M-79-32]$^+$, and [M-79-18-32]$^+$ at m/z 488.39 (RA 5%), 474.37 (RA <1%), and 456.36 (RA 1%); and [M-107-18]$^+$, [M-107-32]$^+$, and [M-107-18-32]$^+$ at m/z 460.39 (RA 2%) 446.38 (RA <1%) and 428.37 (RA <2%), respectively.

The C_{24} bile acid 3β-hydroxychol-5-en-24-oic acid, its [2,2,4,4,23-$^2H_5$] isotopomer and glycine conjugate, and also 3β,7α-dihydroxychol-5-en-24-oic acid, were oxidized with cholesterol oxidase, reacted with GP hydrazine, and analyzed by ES mass spectrometry. Oxidation of these bile acids with cholesterol oxidase results in conversion of the 3β-hydroxyl group to a ketone, and movement of the $\Delta^{5(6)}$ double-bond to $\Delta^{4(5)}$. In this translocation one of the deuterium atoms on C-4 of the deuterated isotopomers is lost to give a mass increase overall of 4 Da (i.e., [2,2,4,23-$^2H_4$]) compared to the unlabeled isotopomer (other isotopomers present include [$^2H_3$] and [$^2H_5$], and to a lesser extent [$^2H_1$] and [$^2H_6$]). The CID spectrum of BA^4-3-one (**XXII**) showed the classical fragmentation pattern of a 3-oxo-Δ^4 GP hydrazone. The interpretation of this CID spectrum was then confirmed by recording the analogous spectrum of the [2,2,4,23-$^2H_4$] isotopomer (**XXIII**) (see Supplementary Material Figure S-3). As anticipated $^\#b_1$-12, $^\#b_2$-CH_2/$^\#b_2$-C_2H_4, and $^\#b_2$ ions were shifted up in mass by 3 Da, as were $^*b_1$-12, $^*b_2$-CH_2/$^*b_2$-C_2H_4 and $^*b_2$ ions (Scheme **3**). Notably, $^*c_2$ was also observed shifted up by 3 Da from m/z 231.15 to 234.17. The glycine conjugate of the [2,2,4,23-$^2H_4$] isotopomer gave a similar series of fragment ions. Due to the inhomogeneity of isotopomers of [$^2H_4$]BA^4-3-one and its glycine conjugate, many fragments were observed as +2 and +3 Da doublets. Incorporation of a 7α-hydroxy group in the bile acid structure, results in a change in the pattern of B-ring fragments. As was the case with other 7-hydroxy-3-oxo-Δ^4-GP hydrazones, in the CID spectrum of BA^4-7α-ol-3-one (**XXV**) the B-ring fragment ion peaks $^\#b_2$-CH_2 (m/z 135.09), $^\#b_2$ (m/z 149.11), $^*b_2$-CH_2 (m/z 163.09) and $^*b_2$ (m/z 177.10) are attenuated, while peaks at 123.09 ($^\#b_1$-12), 151.09 ($^\#b_3$-C_2H_4/$^*b_1$-12) and 179.08 ($^*b_3$-C_2H_4) are accentuated. Again the presence of the labile 7α-hydroxy group had the effect of enhancing the intensity of [M-79-18]$^+$ and [M-107-18]$^+$ ions.

When 22-oxocholesterol was oxidized with cholesterol oxidase and treated with GP hydrazine, two major peaks were observed in the ES mass spectrum at m/z 532.39 and 333.23. The peak at 532.39 corresponds to the mono-GP hydrazone (**X**) and that at 333.23 to the doubly charged bis-GP hydrazone (**XI**). CID of the mono-GP hydrazone gives the expected series of ring fragments for a 3-oxo-Δ^4 3-GP hydrazone, i.e., $^\#b_1$-12 (123.09), $^\#b_2$-CH_2/$^\#b_3$-C_2H_4 (135.09), $^\#b_2$ (149.11), $^*b_1$-12

(151.09), *b_2-CH_2/*b_3-C_2H_4 (163.09), *b_2 (177.10), and *c_2 (231.15); but with enhanced abundance of fragment ions at 282.22 ($C_{20}H_{28}N$), 297.23 ($C_{20}H_{29}N_2$), 312.27 ($C_{22}H_{34}N$), 325.23 ($C_{21}H_{29}N_2O$), 327.28 ($C_{22}H_{35}N_2$), and 355.27 ($C_{23}H_{35}N_2O$) corresponding to #e-H-NH, #e-H, #f + H-NH, *e-H, #f + H and *f+ H or #g + H, respectively (Figure 2f). Both *f + H and #g + H fragments have the elemental composition $C_{23}H_{35}N_2O$. The absence of an ion at m/z 355.27 in the CID spectrum of the [M-107]$^+$ ion, but the presence of an ion at m/z 327.28 correspond-ing to the #f + H fragment in the spectrum (data not shown), strongly suggests that the ion of m/z 355.27 in the spectrum of the [M]$^+$ ion corresponds to a *f + H fragment. In the low mass range of the spectrum, the usual pattern of fragment ions at m/z 80.05, 94.07, 108.08, 109.08, 120.05/120.08 and 137.07 is distorted by the presence of ions at m/z 81.07 and 99.08. These ions correspond to hydrocarbon fragments with chemical formulas C_6H_9, and $C_6H_{11}O$ formed by cleavage of the C-20–C-22 bond α to the carbonyl group at C-22. The C_6H_9 (F-H_2O) fragment is probably derived by water loss from $C_6H_{11}O$ (F) (Scheme 5). The structural signif-icance of these low-mass fragment ions observed in the CID spectrum of C^4-3,22-dione 3-GP hydrazone encour-aged us to reinspect the low mass regions of our spectra (see below).
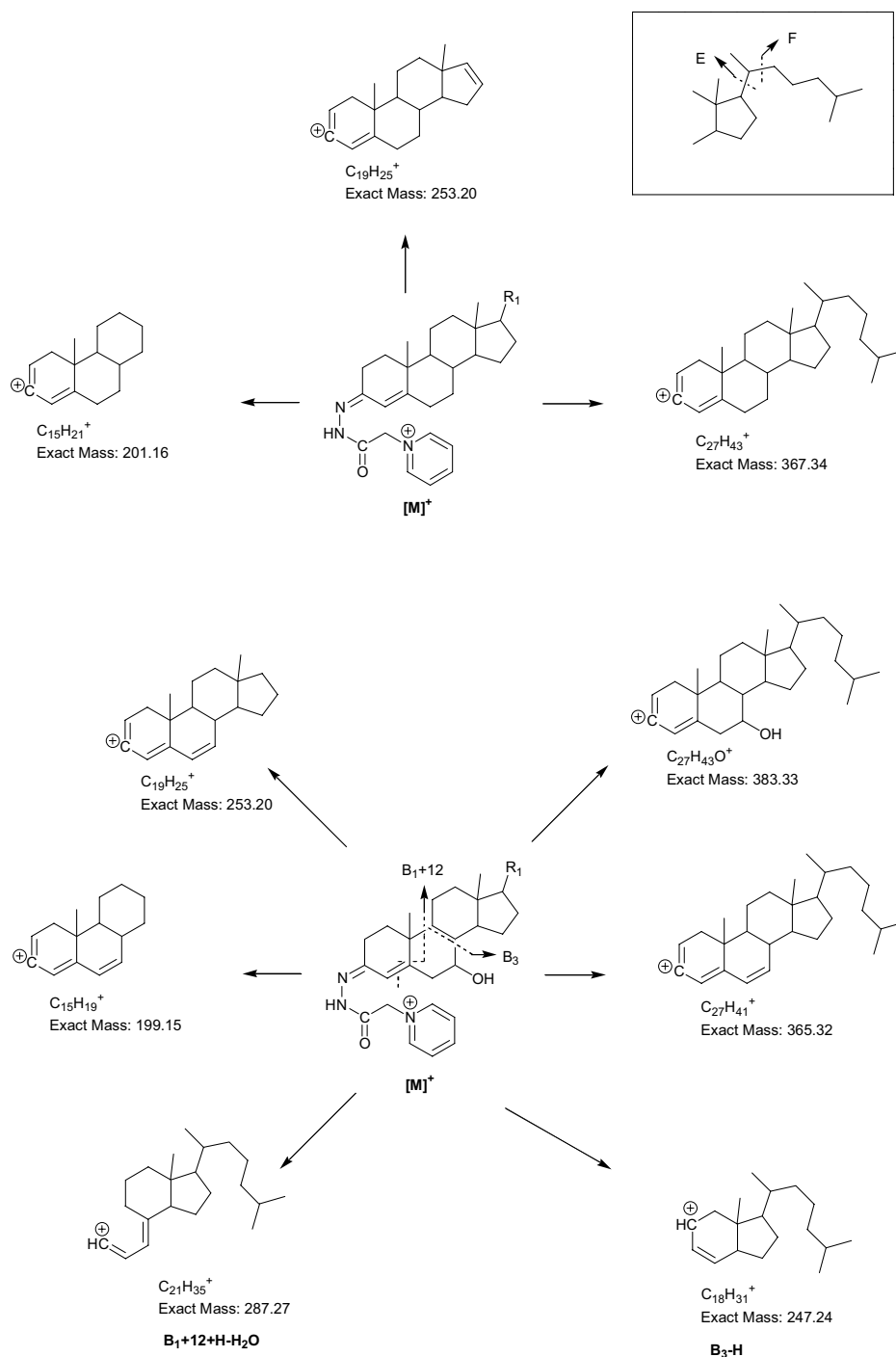
In the CID spectrum of the [M]$^{2+}$ ion of the bis-GP hydrazone (XI) the low mass range is also different to that normally observed for a 3-oxo-Δ^4 GP hydrazone, in that additional peaks are observed at m/z 91.05 (C_7H_7) and 112.11 ($C_7H_{14}N$). The characteristic #b_1-12 (123.09), #b_2-CH_2/#b_3-C_2H_4 (135.09), *b_1-12 (151.09), and *b_2-CH_2/*b_2-C_2H_4 (163.09) ions are observed, but are of minor abundance. The presence of the substituent on C-22 facilitates cleavage of the C-20–C-22 bond with the formation of a *f-H (353.26) fragment. The spectrum is dominated by fragment ions formed by losses from the GP hydrazone group giving doubly charged ions at m/z 293.71 ([M-79]$^{2+}$, $C_{36}H_{53}N_5O_2$), 279.71 ([M-107]$^{2+}$, $C_{35}H_{53}N_5O$), 254.19 ([M-(79 × 2)]$^{2+}$, $C_{31}H_{48}N_4O_2$) and 240.19 ([M-79-107]$^{2+}$, $C_{30}H_{40}N_4O$). Complementary sin-gly charged ions are observed at 586.41 ([M-80]$^+$, $C_{36}H_{52}N_5O_2$) and 507.37 ([M-79-80]$^+$, $C_{31}H_{47}N_4O_2$), and additional singly charged fragments are observed at 544.40 ([M-122]$^+$, $C_{34}H_{50}N_5O$), 543.41 ([M-107-16]$^+$, $C_{35}H_{51}N_4O$), 516.40 ([M-150]$^+$, $C_{34}H_{50}N_3O$), 465.36 ([M-107-94]$^+$, $C_{29}H_{45}N_4O$), 464.36 ($C_{30}H_{46}N_3O$), and 437.35 ([M-79-150]$^+$, $C_{29}H_{45}N_2O$).

Group (iv) fragment ions: Hydrocarbon ions. To aid the interpretation of the hydrocarbon fragment ion pattern formed by 3-oxo-Δ^4 sterol GP hydrazones it is advanta-geous to consider the CID spectra of the simplest C_{27} steroid, i.e., C^4-3-one GP hydrazone (I) (Figure 3c), and of a simple C_{19} steroid, i.e., A^4-17β-ol-3-one GP hydrazone (XXVI) (spectrum not shown). Peaks at m/z 81.07 (C_6H_9), 93.07 (C_7H_9), 95.09 (C_7H_{11}), 105.07 (C_8H_9), 107.09 (C_8H_{11}), 109.10 (C_8H_{13}), and 119.09 (C_9H_{11}) are observed in both spectra indicating that they are derived from the steroid

ring system. There is enhanced intensity at m/z 95.09, 107.09 and 109.10 and an additional peak at 111.12 (C_8H_{15}) in the spectrum of C^4-3-one GP hydrazone demonstrating that these peaks are additionally derived from the side-chain. At higher mass, fragment ions are observed at 201.16 ($C_{15}H_{21}$), and 253.20 ($C_{19}H_{25}$) in the spectrum of A^4-17β-ol-3-one corresponding to the doubly unsaturated ABC ring system, and the triply unsaturated steroid ABCD-ring system plus C-18 and C-19, respectively, (Scheme 5). These ions are present in the spectrum of C^4-3-one GP hydrazone, but are of low abundance, in-stead a fragment ion is observed at 367.34 ($C_{27}H_{43}$) corre-sponding to the cholestane skeleton with two double bonds. Compared with this template, the CID spectra of 3-oxo-Δ^4 sterol GP hydrazones show many similarities.

The isomers of monohydroxylated C^4-3-one GP hydra-zone (V–IX) show the same pattern of low mass fragments as C^4-3-one GP hydrazone (Figure 2a–e). At higher mass peaks at m/z 199.15 ($C_{15}H_{19}$), 253.20 ($C_{19}H_{25}$) and 365.32 ($C_{27}H_{41}$) are observed consistently; while a peak at m/z 383.33 ($C_{27}H_{43}O$) corresponding to doubly unsaturated cholestanol is observed in the spectra of the 7β-hydroxy- and 27-hydroxy-isomers (Scheme 5). The 7-hydroxy iso-mer additionally gives fragment ions at m/z 247.24 ($C_{18}H_{31}$, B_3-H), and 287.27 ($C_{21}H_{35}$, B_1 + 12 + H-H_2O) (Scheme 5). These ions are complementary to b_3-type and b_1-12 type fragments respectively, and their formation is encouraged by the presence of the 7β-hydroxyl group. The dihydroxylated versions of C^4-3-one carrying hy-droxyl groups in the side-chain and at C-7 give essentially the same pattern of low mass fragment ions as their monohydroxy analogs, this is also true in the higher mass range, however, the peak at m/z 365.32 is now shifted to 363.31 ($C_{27}H_{39}$), that at 383.33 to 381.32 ($C_{27}H_{41}O$), and that at 247.24 to 245.23 ($C_{18}H_{29}$, B_3-H-H_2O), while the peak at m/z 287.27 is no longer observed (Figure 3a, and Supplementary Material Figure S-1). Incorporation of two hydroxyl groups on the side-chain as in C^4-20R,22R-diol-3-one (XII), has a major effect on the pattern of low mass hydrocarbon fragment ions (Figure 3b). In the low mass range, the dominant fragment ion is now at 109.10 (C_8H_{13}); this is more intense than the fragment ions at m/z 94.07 (σ_2 + H, C_6H_8N), 108.08 ($C_7H_{10}N$), and 120.05 (σ_3-H, C_7H_6NO), which normally dominate this region of the spectrum. The ion at m/z 109.10 (C_8H_{13}) corresponds to a doubly unsaturated side-chain fragment formed by cleav-age of the C-17–C-20 bond α to the C-20 hydroxyl group, i.e., E-(2xH_2O). In the higher mass range essentially only the hydrocarbon fragment ion at 253.20 ($C_{19}H_{25}$) is observed.

As discussed above, the low mass pattern of fragment ions is distorted in the CID spectra of C^4-3,22-dione 3-GP hydrazone (X) (Figure 2f). Ions at m/z 81.07 (C_6H_9) and 99.08 ($C_6H_{11}O$) corresponding to fragments formed by cleavage of the C-20–C-22 bond α to the carbonyl group now dominate this region of the spectrum. The C_6H_9 fragment is probably derived by water loss from $C_6H_{11}O$.

C$_{19}$H$_{25}^+$
Exact Mass: 253.20

C$_{15}$H$_{21}^+$
Exact Mass: 201.16

C$_{27}$H$_{43}^+$
Exact Mass: 367.34

[M]$^+$

C$_{19}$H$_{25}^+$
Exact Mass: 253.20

C$_{27}$H$_{43}$O$^+$
Exact Mass: 383.33

C$_{15}$H$_{19}^+$
Exact Mass: 199.15

C$_{27}$H$_{41}^+$
Exact Mass: 365.32

C$_{21}$H$_{35}^+$
Exact Mass: 287.27
B$_1$+12+H-H$_2$O

C$_{18}$H$_{31}^+$
Exact Mass: 247.24
B$_3$-H

[M]$^+$

Scheme 5. Hydrocarbon fragment ions formed from 3-oxo-Δ^4 steroid 3-GP hydrazones. The presence of a hydroxyl group on the C-17 side-chain will result in additional unsaturation and a reduction in fragment ion mass by 2.02 Da.

Cholesterol, Cholestadienes, and Side-Chain Modified Cholesterols: Compounds I–IV (see Table 1)

During the analysis of oxysterols from biological sources possibly the oxysterol fractions may be contaminated with cholesterol, its precursors, and possibly by plant sterols present from the diet. We have thus oxidized and derivatized cholesterol, its precursor des-

mosterol (C^{5,24}-3β-ol), and the plant sterols stigmasterol (24β-ethyl-cholesta-5,22-dien-3β-ol, C^{5,22}-24β-ethyl-3β-ol), and sitosterol (24β-ethyl-cholest-5-en-3β-ol, C^5-24β-ethyl-3β-ol) and analyzed their GP hydrazones.

Desmosterol is a precursor in the de novo synthesis of brain cholesterol [54]. When oxidized with cholesterol oxidase and derivatized with GP hydrazine, CID of the resulting C^{4,24}-3-one GP hydrazone (**II**) gives a
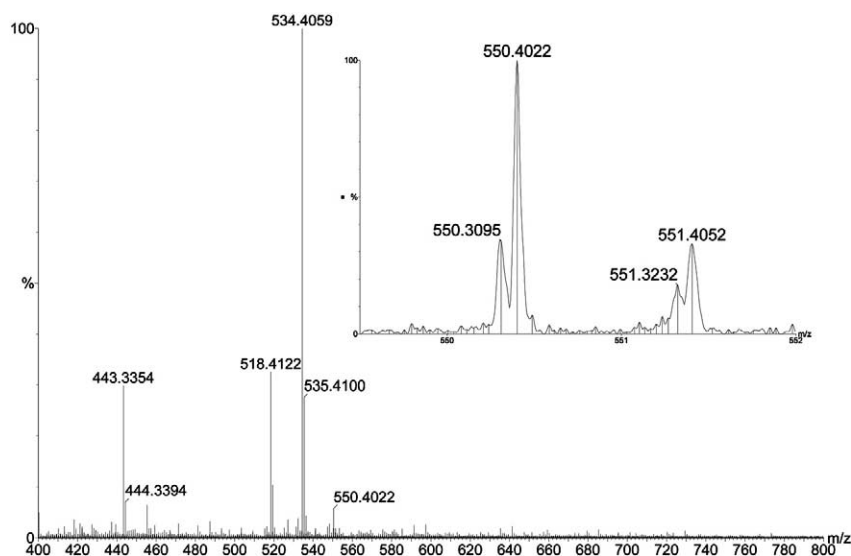
Figure 4. Mass spectrum of the oxidized and derivatized oxysterol fraction of rat brain. The amount of sample loaded into the ES-capillary corresponded to ~40 μg of brain. Spectrum recorded on the Q-TOF Global instrument in "W-mode". The y axis represents relative abundance.

spectrum essentially similar to those of other 3-oxo-Δ^4 steroids (see Supplementary Material Figure S-4). However, peaks at 353.26 ($C_{23}H_{33}N_2O$) and 355.27 ($C_{23}H_{35}N_2O$) corresponding to *f-H and *f + H; and 325.26 ($C_{22}H_{33}N_2$) and 327.28 ($C_{22}H_{35}N_2$) correspond to #f-H and #f + H, are of elevated intensity. These ions are formed by cleavage of the bond between C-20 and C-22 with hydrogen transfer from (f-H), and to (f + H), the ionic fragment.

The level of the plant sterol sitosterol in serum is often used as a marker for cholesterol absorption. Sterol esters, including those of sitosterol and stigmasterol, are present in phytosterol ester enriched low-fat food products, and their consumption has been shown to reduce serum total and LDL cholesterol levels [55, 56]. Conversely, phytosterol levels in plasma become elevated upon consumption of these foods [55]. The CID spectra of C^4-24β-ethyl-3-one (**III**) and $C^{4,22}$-24β-ethyl-3-one (**IV**) GP hydrazones showed the common features of 3-oxo-Δ^4 GP hydrazones (Figure 3d and Supplementary Material Figure S-4). The spectrum of C^4-24β-ethyl-3-one (**III**) was very similar to that of C^4-3-one (**I**), however, the peak at 367.34 ($C_{27}H_{43}$) in the spectrum of C^4-3-one, and corresponding to the doubly unsaturated cholestane skeleton (Scheme **5**), was shifted to 395.37 ($C_{29}H_{47}$) in the spectrum of the 24β analog. The presence of the C-22 – C-23 double-bond in $C^{4,22}$-24β-ethyl-3-one (**IV**) is reflected in the low-mass region of the MS/MS spectrum where the intensity of the ion at m/z 83.09 (C_6H_{11}) is greatly enhanced (Figure 3d). This ion is formed by cleavage of the C-23–C-24 bond α to the C-22–C-23 double-bond. The C-22–C-23 double-bond also has an effect on other side-chain fragmentations. As in the spectrum of C^4-20R,22R-diol-3-one GP hydrazone (**XII**) (Figure 3b), there is enhanced abundance of fragment ions at m/z 284.24 ($C_{20}H_{30}N$, #e + H-NH),

299.25 ($C_{20}H_{31}N_2$, #e + H), and 327.24 ($C_{21}H_{31}N_2O$, *e + H), each formed as a result of cleavage of the C-17–C-20 bond, and in the case of $C^{4,22}$-24β-ethyl-3-one (**IV**), β to the double-bond. It is interesting to note that a similar triad of fragment ions is observed in the spectrum of C^4-3,22-dione 3-GP hydrazone (**X**) but shift to lower mass by 2 Da (Figure 2f). The CID spectrum of $C^{4,22}$-24β-ethyl-3-one is further characterized by peaks at 353.30 ($C_{24}H_{37}N_2$, #h + H), and 381.29 ($C_{25}H_{37}N_2O$, *h + H) both formed as a result of cleavage of the C-23–C-24 bond.

Oxysterols in Brain

To evaluate the analytical method described above the oxysterol content of rat brain was investigated. Oxysterols in rat brain were extracted [36, 37], oxidized with cholesterol oxidase, and derivatized to GP hydrazones. The method has yet to be fully optimized and further details of the extraction procedure will be published when appropriate. Shown in Figure 4 is the ES mass spectrum of the oxidized and derivatized oxysterol fraction of rat brain. The amount of sample loaded into the ES-capillary corresponded to ~40 μg of brain. A major peak is observed at m/z 534.41, which corresponds to the m/z of the $[M]^+$ ion of a monohydroxy-3-oxo-Δ^4 C_{27} steroid GP hydrazone. MS/MS of the ion at m/z 534.41 gave the spectrum shown in Figure 2b. The low-mass pattern of fragments at m/z 80.05, 94.07, 108.08, 109.08, 120.05, and 137.07, and the high-mass pattern at 455.36 ($[M-79]^+$) and 427.37 ($[M-107]^+$), confirmed that the precursor ion corresponded to a GP hydrazone. The fragment ion pattern 123.09 (#b$_1$-12), 135.09 (#b$_2$-CH$_2$/#b$_3$-C$_2$H$_4$), 149.11 (#b$_2$), 151.09 (*b$_1$-12), 163.09 (*b$_2$-CH$_2$/*b$_2$-C$_2$H$_4$), and 177.10 (b$_2$) are indicative of a 3-oxo-Δ^4 GP hydrazone unsubstituted at posi-

tion C-7 (cf. Figure 2a). Fragment ions are additionally observed at 231.15 (*c_2), 285.20 (*d_1), 325.23 (*e-H), 325.26 (#f-H), 327.24 (*e + H), and especially at 353.26 (*f-H), which are consistent with a 24-hydroxycholest-4-en-3-one GP hydrazone (VI) structure. 24-Hydroxy-cholest-4-en-3-one is the product of cholesterol oxidase mediated oxidation of 24-hydroxycholesterol. The identification of 24-hydroxycholesterol in brain is in agreement with the work of Smith and colleagues who showed in 1973 that 24-hydroxycholesterol is the major oxysterol in brain [57], and of Björkhem and colleagues who have shown that in rat about 70% of the 24S-hydroxycholesterol in plasma is of cerebral origin [58]. Exact mass measurements made in the ES mass spectrum shown in Figure 4 suggest the presence of a second 3-oxo-Δ^4-steroid GP hydrazone at m/z 550.40. A mass of 550.40 Da corresponds to a dihydroxy-3-oxo-Δ^4 C_{27} steroid GP hydrazone, and CID of the ion at m/z 550.40 gives a spectrum indicative of a dihydroxy-3-oxo-Δ^4 C_{27} steroid GP hydrazone, with probably the two hydroxyl groups on the C-17 side-chain (see Supplementary Material Figure S-1f), but not a 20,22-diol. Many peaks in the CID spectrum of m/z 550.40 are not easily explained by a single dihydroxy-3-oxo-Δ^4 C_{27} steroid GP hydrazone structure, and it seems likely that more than one compound (isomer) is being subjected to MS/MS. It should be noted, that to obtain sufficient precursor-ion current the resolution of the quadrupole was reduced so as to allow transmission of an m/z window of about 2 units. Significantly, the fragment ions at m/z 120.05 (σ_3-H), and 137.07 (σ_4 + H) are more abundant than is normally the case with 3-oxo-Δ^4-steroids, and additional fragment ions are observed at 167.12 and 181.13 of unknown origin.

Zhang et al. have demonstrated the conversion of 24-hydroxycholesterol to 24,25-dihydroxycholesterol in cultures of fetal rat astrocytes [59]. In the same study, they showed that 24-hydroxycholesterol is not 7-hydroxylated in these cultures, and it has subsequently been confirmed that CYP7B1 does not 7-hydroxylate 24-hydroxycholesterol. The possibility exists that the 24,25 diol is cleaved by oxidation into a C-24 acid. In brain this would lead to the cholenoic acid that can be 7-hydroxylated [60]. More recently, Mast et al. [61] have shown that CYP46A1, the enzyme responsible for 24S-hydroxylation of cholesterol in brain, can further metabolize 24S-hydroxycholesterol to 24,25- and 24,27-dihydroxycholesterol in cell cultures transfected with human CYP46A1 cDNA and in an vitro reconstituted system with recombinant enzyme. In vivo studies on the metabolism of 24-hydroxycholesterol in humans have shown that 27-hydroxylation, formation of bile acids and double conjugation are the main pathways of metabolism in man [25].

The apparent inhomogeneity of the precursor ion at m/z 550 emphasizes the importance of the incorporation of a LC step before mass analysis so as to resolve isomeric compounds in the time domain. Procedures to analyze oxysterol GP hydrazones by capillary-LC-

MS/MS using the Q-TOF instruments and the triple quadrupole are currently being studied in our laboratories, and we show only preliminary data here.

Using the C_{18} capillary column with gradient elution we are able to separate the reference monohydroxy-3-oxo-Δ^4 C_{27} steroid GP hydrazones. When the brain sample was injected onto the column following oxidation and derivatization, only one chromatographic peak was observed to corresponding to a monohydroxy-3-oxo-Δ^4 C_{27} steroid GP hydrazone (M^+, m/z 534.41) (Figure 5a). The retention time for this compound was identical to that of reference C^4-24S-ol-3-one GP hydrazone (VI, 21.04 min) and it gave an MS/MS spectrum consistent with this structure (cf Figure 5a inset, Figure 2a and b). Dihydroxy-3-oxo-Δ^4 C_{27} steroid GP hydrazones give an M^+ ion at m/z 550.40. A reconstructed ion chromatogram (RIC) for this ion in the brain sample gave at least four chromatographic peaks (Figure 5b), one of which gave an MS/MS spectrum of a dihydroxy-3-oxo-Δ^4 C_{27} steroid GP hydrazones where both hydroxyl groups are probably on the C-17 side-chain (Figure 5b).

Discussion

Fragmentation of 3-Oxo-Δ^4 Steroids and Their Cationic Derivatives

The fragmentation reactions of 3-oxo-Δ^4 steroids, their 3-oxime, and Girard hydrazone derivatives have previously been investigated [38–40, 49, 50, 52]. There is general agreement as to the structure of the b_1-12 and b_2 type ions, but some debate as to the structure of the b_2-CH_2 type ions [53]. The use of deuterium labeled steroids in this current study provide further evidence for the b_1-12 type ions to consist of the steroid A-ring plus C-19 but minus C-5; and the b_2 type ions to consist of the A ring, C-6 and C-19 (Scheme 3). The structure of the b_2-CH_2 type ions is less clear-cut. After performing detailed stable-isotope labeling studies Liu et al. [49] proposed that these ions contain the A-ring and C-6, but that C-19 has been lost and replaced by H-atom from C-7 or the CD-rings. In addition, the 6β-H has been replaced by an H-atom from C-7 or the CD-rings. A better description for these types of ions is thus b_2-CH_3-H + 2H (Scheme 3). In contrast to this explanation, Williams et al. [52] in their study of testosterone and hydroxylated versions thereof proposed that Liu's b_2-CH_2 ions consist of the A-ring, plus C-6 and C-7 but minus C-10 and C-19 and a H-atom from C-6. (Scheme 3), and are thus better described as b_3-C_2H_4 ions. In the current study, when a 7-hydroxyl group was incorporated into the 3-oxo-Δ^4 structure, GP hydrazone fragment ions were observed at m/z 135.09 and 163.09, corresponding to ions with the elemental composition $C_8H_{11}N_2$ (#b_2-CH_2) and $C_9H_{11}N_2O$ (*b_2-CH_2), respectively, but at reduced abundance (Figure 2). According to Liu's structure, such ions would be better described as b_2-CH_3-H + 2H type ions. Williams' b_3-C_2H_4 type
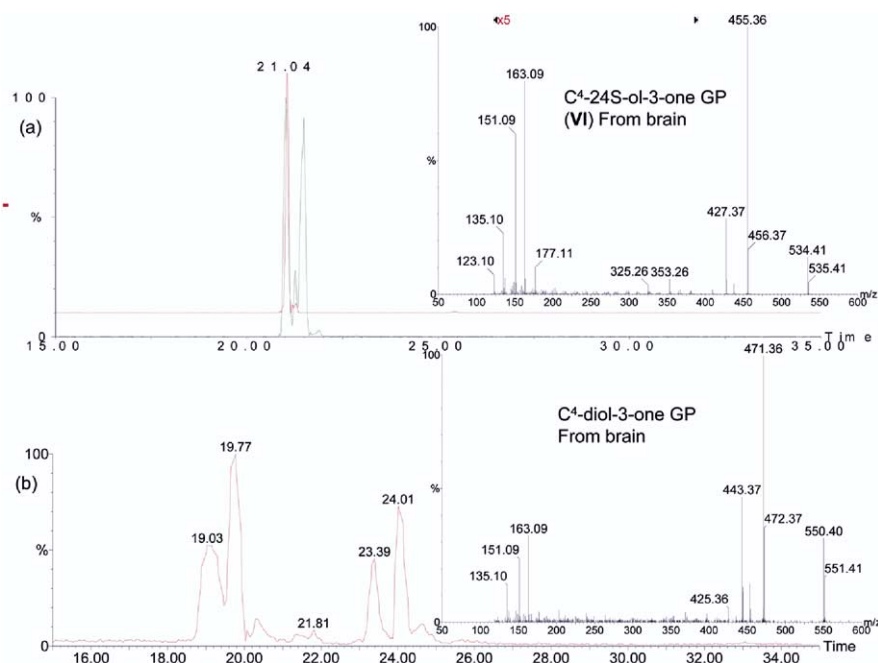
Figure 5. (**a**) RICs for a reference mixture of C^4-24S-ol-3-one GP and C^4-24R-ol-3-one GP (green lower trace); and C^4-24S-ol-3-one GP (red upper trace) from the brain sample after oxidation and derivatization. The inset shows the MS/MS spectrum of m/z 534.41 (retention time 21.04 min) from brain. (**b**) RIC for m/z 550.40 from the brain sample following oxidation and derivatization. The inset shows the MS/MS spectrum of m/z 550.40 eluting at 19.03 min. Spectra were recorded on the Q-TOF Global in the "V-mode".

ions would not have m/z values of 135.09 and 163.09, but rather 151.09 ($C_8H_{11}N_2O$) and 179.08 ($C_9H_{11}N_2O_2$), respectively. Thus, the observation of fragment ions at m/z 135.09 and 163.09 in the spectra of 7-hydroxy-3-oxo-Δ^4 steroids indicates that a reaction channel exists for the formation of ions with Liu's b_2-CH_3-H + 2H structure (Figure 2e, Scheme 3). The presence of a 7-hydroxyl group on the steroid skeleton does results also in the formation of fragment ions at m/z 179.08, these ions could be formed by cleavage between C-6 and C-7 with the accompanying loss of C-19 and 6β-H, but with the gain of a H-atom from the CD ring and an OH group from C-7, i.e., *b_2-CH_3-H + H + OH (Figure 2e, Scheme 3). Alternatively, the ion at m/z 179.08 could simply be of the structure *b_3-C_2H_4 as suggested by Williams et al. The equivalent #b_2-CH_3-H + H + OH and #b_3-C_2H_4 ions appear at m/z 151.09, as do *b_1-12 ions. The dominant b-type ions in the CID spectra of 7-hydroxy-3-oxo-Δ^4 steroid GP hydrazones appear at m/z 123.09 ($C_7H_{11}N_2$, #b_1-12) and 151.09 ($C_8H_{11}N_2O$, *b_1-12 or *b_2-CH_3-H + H + OH and #b_3-C_2H_4) (Figures 2e, 3a, and Supplementary Material Figure S-1). This prominence of b_1-12 type ions can be explained by the lability of the C-7 hydroxyl group and its propensity to eliminate as water and generate a double-bond between C-6 and C-7, thereby attenuating alternative b-type fragmentation channels. The overriding abundance of the ion at m/z 151.09 is probably a consequence of the fact that different fragment ions, i.e., #b_2-CH_3-H + H + OH, #b_3-C_2H_4, and *b_1-12, each has an identical elemen-

tal composition and a mass of 151.09 and each contributes to the ion current giving this peak.

In summary, the results of the current study indicate that Liu's b_2-CH_3-H + 2H type ions can be formed, but do not allow the differentiation of b_3-C_2H_4 from b_2-CH_3-H + 2H in 3-oxo-Δ^4 steroids without a hydroxyl group at C-7; or b_3-C_2H_4 from b_2-CH_3-H + H + OH in 7-hydroxy-3-oxo-Δ^4 steroids ions. To elucidate further the structure of these ions, 3-oxo-Δ^4 steroids labeled with ^{13}C at C-7 or C-10 should be analyzed.

While the B-ring fragment ions are the dominant cleavage products of the steroid skeleton, fragment ions important in the structural identification of 3-oxo-Δ^4 sterol GP hydrazones are formed by additional cleavage in the C- and D-rings, and in the C-17 side-chain. For example, the enhanced abundance of fragment ions at m/z 325.26 and 353.26 in the CID spectrum of a monohydroxy-3-oxo-Δ^4 C_{27} steroid (m/z 534.41) are indicative of a 24-hydroxyl group, and correspond to #f-H and *f-H fragments (Figure 2a, b, and h upper panels, Figure 5a, Scheme 2). Similarly, the presence of the 25-hydroxyl group in C^4-25-ol-3-one GP hydrazone (**VII**) can be identified by enhanced abundance of #h-H and *h-H ions at m/z 353.30 and 381.29 (Figure 2c, h right central panel), while an abundant ion at 327.24 (*e + H) is indicative of the 27-hydroxyl group (Figure 2d). Although these three isomers, and additionally the 7-hydroxy isomers, can be differentiated at low-resolution on the tandem quadrupole from the above peak patterns, the identity of the fragment ions requires the acquisition of spectra at "moderate"- to "high"-resolution.

The value of recording MS/MS spectra at high-resolution, and the ability to accurately measure peak centroids, is nicely illustrated in the CID spectra C^4-24-ol-3-one GP hydrazone (**VI**, Figures 1 and 2h). Shown in Figure 2h (upper panels) are expanded views of the peaks in the m/z 325 and 353 regions recorded at "high-resolution" ($\sim$ 16,000 FWHM) on the Q-TOF instruments. At this resolution peaks at m/z 325.23 and 325.26 are fully resolved, respectively. By centroiding the respective peaks, elemental compositions of $C_{21}H_{29}N_2O$ (*e-H) and $C_{22}H_{33}N_2$ (#f-H) are determined. Even when spectra are recorded at "moderate" resolution (12,000), the accurate mass values are within 10 ppm of the theoretical mass values for these elemental formulas (data not shown). In the m/z 353 region, just one peak is observed at m/z 353.26 corresponding to an elemental composition $C_{23}H_{33}N_2O$ (*f-H), and not surprisingly the centroid of this fully resolved peak gives good agreement with the theoretical mass (2 ppm). The ability of the Q-TOF instruments to resolve close lying peaks and accurately measure their position on the m/z scale is of great value in identifying ion structure. Further, a knowledge of the elemental composition of the precursor ion (determined in an independent mass scan), e.g., $C_{34}H_{52}N_3O_2$ for C^4-24-ol-3-one GP hydrazone (**VI**), is used to limit the chemical composition of possible fragment ions in a search of measured mass against elemental composition. This improves the specificity of the search, and effectively means that a mass accuracy of 10 ppm can allow the unique identification of most fragment ions.

Most fragment ions in the CID spectra of 3-oxo-Δ^4 GP hydrazones are derived from $[M-79]^+$ or $[M-107]^+$ intermediates (Scheme **2**). Those derived from the $[M-79]^+$ intermediate (indicated by an asterisk) are modified by the addition of the $NNHCOCH_2$ group (71.0245 Da) to the steroid skeleton, while those derived from the $[M-107]^+$ intermediate (indicated by a hatch, #) are modified with a $NNHCH_2$ group (43.0296). These "groups" or "tags" are mass deficient with respect to moieties made up simply of carbon and hydrogen. Taking the $NNHCOCH_2$ (71.0245 Da) tag for example, the hydrocarbon closest in mass is C_5H_{11} at 71.0861 Da, 61.6 mDa (867 ppm) away from the tag. Additionally, the two tags have different degrees of mass deficiency, the result of which is that at a given nominal mass, e.g., 325 (Figure 2h), fragment ions tagged with $NNHCOCH_2$ (i.e., *e-H, 325.2280 Da) are resolved from those tagged with $NNHCH_2$ (i.e., #f-H, 325.2644 Da) or any possible hydrocarbon fragments (i.e., $C_{24}H_{37}$, 325.2895 Da).

As with the monohydroxy-3-oxo-Δ^4 steroids, the MS/MS spectra of the dihydroxy-3-oxo-Δ^4 GP hydrazones studied allowed isomer differentiation. The presence of a 7-hydroxyl group is immediately evident by the altered pattern of B-ring fragments. Somewhat surprisingly, the C^4-7α,25-diol-3-one (**XIII**) isomer gives a noticeably different spectrum to the C^4-7β,25-diol-3-one (**XIV**) isomer (see Supplementary Material Figure

S-1). In the spectrum of the 7α isomer there is enhanced abundance of the fragment ions at m/z 203.15 (#c_2 + 2H-H_2O) and 231.15 (*c_2+2H-H_2O), while in the spectrum of the 7β isomer the fragment ion at 341.22 (*e-H) is enhanced. Significantly, there is also a major difference in the relative abundance of $[M-79-18]^+$ and $[M-107-18]^+$ ions between these isomers, in that the dehydration products (m/z 453.15, 425.35) are more prevalent in the spectrum of the 7β isomer. The presence of the 7α-hydroxyl group in C^4-7α,27-diol-3-one (**XV**) also affects the fragment ion ratio of ions at m/z 203.15, 231.15, and 341.22 in that the abundance of ions at 203.15 and 231.15 are enhanced (Figure 3a). This isomer can then be differentiated from the 7β,25-diol on account of the abundance of these fragment ions, and from the 7α,25-diol on account of the abundance of $[M-79-18]^+$ fragment (m/z 453.35). The presence of the 25-hydroxyl group results in enhanced dehydration of the $[M-79]^+$ fragment ion. The lability of the 25-hydroxyl group also enhances the abundance of fragment ions at m/z 363.31 ($C_{27}H_{39}$) compared with that at 381.32 ($C_{27}H_{41}O$), corresponding to quadruply unsaturated cholestane and triply unsaturated cholestanol skeletons, respectively (cf. Scheme **5**). The MS/MS spectrum of C^4-20R,22R-diol-3-one (**XII**) is quite different from that of isomers possessing a 7-hydroxyl group on account of the pattern of B-ring fragments. Additionally, the presence of the 20,22-diol structure gives enhanced abundance of ions at m/z 299.25 (#e + H), 327.24 (*e + H) and 353.26 (*f + H-H_2O) (Figure 3b). The 20,22-diol structure is further characterized by an abundant fragment ion at m/z 109.10 (C_8H_{13}). This ion corresponds to a side-chain fragment formed by cleavage of the C-17–C-20 bond, and which is additionally doubly unsaturated by loss of the two water molecules. This ion is complementary to e-type fragments. The absence of an abundant ion at m/z 109.10 in the MS/MS of the dihydroxy-3-oxo-Δ^4 steroid GP hydrazone in the brain sample analyzed (Figure 5b and Supplementary Material Figure S-1f) argues against it being a 20,22-diol, and the pattern of B-ring fragment ions definitely indicates that the steroid is not 7-hydroxylated. We tentatively suggest a 24,25-diol, a 24,27-diol or a 25,27-diol structure (Figure 5b and Supplementary Material Figure S-1f). The presence of multiple isomers in the brain sample emphasizes the importance of incorporation of the LC-MS/MS step (Figure 5).

Although only one dioxosteroid was analyzed in the current study, i.e., C^4-3,20-dione, the MS/MS spectra of both the bis- and mono-GP hydrazones (**X**, **XI**) give fragment ion information which aid in the location of the two oxo groups. In earlier studies, we have observed that GP hydrazine reacts faster with the 3-oxo-Δ^4 structure than with simple ketones, and the MS/MS spectrum of the C^4-3,22-dione mono-GP (**X**) confirms this, i.e., the pattern of b_1-12, b_2-CH_2/b_3-C_2H_4 and b_2 B-ring fragment ions is observed (Figure 2f). Additionally, the location of the C-22 ketone is indicated by the abundant #e-H and *e-H fragments (m/z 297.23, 325.23)

formed by a McLafferty-type fragmentation of the bond β to the ketone group. The low-mass region of the spectrum also gives fragment ions indicative of the 22-oxo group, i.e., at m/z 99.08, ($C_6H_{11}O$, F) and 81.07, (C_6H_9, F-H_2O). These are cations formed by cleavage of the C-20–C-22 bond α to the ketone group, without and with dehydration (cf. Scheme **5**). The observation of these structurally informative low-mass fragment-ions emphasizes the importance of recording the entire MS/MS spectrum, not just a portion of it (cf. ion-trap data). Inspection of the MS/MS spectrum of the bis-derivative (Figure 2g) reveals a very minor pattern of B-ring fragments, and a structurally significant fragment at m/z 353.26 (*f-H) formed by cleavage of the C-20–C-22 bond. Most of the spectrum is dominated by fragment ions formed by cleavages through the hydrazone groups, which are less structurally informative, but are of value for neutral-loss scanning.

The low-mass region of the MS/MS spectra of steroid GP hydrazones is particularly informative when the C-17 side-chain contains two hydroxyl groups (Figure 3b), or an unsaturated group. This is evident in the spectra of C^4-3,22-dione (**X**) and $C^{4,22}$-24β-ethyl-3-one (**IV**) (Figures 2f, 3d). The presence of the C-22–C-23 double-bond in the $C^{4,22}$-24β-ethyl-3-one (**IV**) structure results in an abundant fragment at m/z 83.09 (C_6H_{11}) formed by cleavage of the C-23–C-24 bond.

Sensitivity of Analysis

Without derivatization, oxysterols are difficult to analyze by mass spectrometry. Traditionally, oxysterols are analyzed by GC-MS after derivatization of the hydroxyl groups to trimethylsilyl ethers [31, 32]; alternatively cholesterol-like molecules can be analyzed by ES-MS and ES-MS/MS after one of a number of different derivatization reactions [53]. In the current study, molecules with a C^5-3β-ol structure have been oxidized to 3-oxo-Δ^4 steroids and then derivatized to GP hydrazones. Steroids with C^5-3β-ol structure are extremely insensitive to ES ionization, and are only observed on the 100 ng level, 3-oxo-Δ^4 steroids give $[M + H]^+$ ions and can be observed on the 500 pg level, but further derivatization to their GP hydrazones gives sub-pg sensitivity.

As with all analytical methods, there are advantages and disadvantages; in an attempt to provide an even handed discussion we draw the attention of the reader to the following: Only 3β-hydroxy-Δ^5 and 3β-hydroxy-5α steroids are oxidized by cholesterol oxidase, however, steroid dehydrogenases are available that can be used for other isomers. Oxysterols with a second substituent in the A-ring are oxidized slowly or perhaps not at all by cholesterol oxidase. Polyketonic oxysterols may give multiple derivatives with one or several GP groups; oxysterols containing an oxo group formed in vitro should then be analyzed before and after treatment with cholesterol oxidase.

The true value of the current procedure is most effectively illustrated by the fact that a high quality MS/MS spectrum of oxidized and derivatized 24-hydroxycholesterol were obtained when a sample corresponding to oxysterols extracted from only 40 μg of brain tissue was loaded into the ES capillary or onto C_{18} capillary column. When the extraction, oxidation and derivatization procedures have been fully optimized it can be expected that the amount of tissue required could be reduced further. This degree of sensitivity makes oxysterol analysis from tissue biopsies a real possibility.

Acknowledgments

References

1. Björkhem, I.; Meaney, S.; Diczfalusy, U. Oxysterols in human circulation: Which role do they have? *Curr. Opin. Lipidol.* **2002,** *13,* 247–253.
2. Björkhem, I.; Diczfalusy, U. Oxysterols, friends, foes, or just fellow passengers? *Arterioscler. Thromb. Vasc. Biol.* **2002,** *22,* 734–742.
3. Axelson, M.; Mörk, B.; Sjövall, J. Occurrence of 3β-hydroxy-5-cholestenoic acid, 3β,7α-dihydroxy-5-cholestenoic acid, and 7α-hydroxy-3-oxo-4-cholestenoic acid as normal constituents in human blood. *J. Lipid Res.* **1988,** *29,* 629–641.
4. Zhang, J.; Larsson, O.; Sjövall, J. 7α-Hydroxylation of 25-hydroxycholesterol and 27-hydroxycholesterol in human fibroblasts. Biochim. Biophys. Acta **1995,** *1256,* 353–359.
5. Lund, E.; Andersson, O.; Zhang, J.; Babiker, A.; Ahlborg, G.; Diczfalusy, U.; Einarsson, K.; Sjövall, J.; Björkhem, I. Importance of a novel oxidative mechanism for elimination of intracellular cholesterol in humans. *Arterioscler. Thromb. Vasc. Biol.* **1996,** *16,* 208–212.
6. Meaney, S.; Bonfield, T. L.; Hansson, M.; Babiker, A.; Kavuru, M. S.; Thomassen, M. J. Serum cholestenoic acid as a potential marker of pulmonary cholesterol homeostasis : Elevated levels in patients with pulmonary alveolar proteinosis. *J. Lipid Res.* **2004,** *45,* 2354–2360.
7. Babiker, A.; Andersson, O.; Lindblom, D.; van der Linden, J.; Wiklund, B.; Lutjohann, D.; Diczfalusy, U.; Bjorkhem, I. Elimination of cholesterol as cholestenoic acid in human lung by sterol 27-hydroxylase: Evidence that most of this steroid in the circulation is of pulmonary origin. *J. Lipid Res.* **1999,** *40,* 1417–1425.
8. Schroepfer, G. J. Oxysterols: Modulators of cholesterol metabolism and other processes. *Physiol. Rev.* **2000,** *80,* 361–554.
9. Lehmann, J. M.; Kliewer, S. A.; Moore, L. B.; Smith-Oliver, T. A.; Oliver, B. B.; Su, J. L.; Sundseth, S. S.; Winegar, D. A.; Blanchard, D. E.; Spencer, T. A.; Willson, T. M. Activation of the nuclear receptor LXR by oxysterols defines a new hormone response pathway. *J. Biol. Chem.* **1997,** *272,* 3137–3140.
10. Janowski, B. A.; Willy, P. J.; Devi, T. R.; Falck, J. R.; Mangelsdorf, D. J. An oxysterol signalling pathway mediated by the nuclear receptor LXRα. *Nature* **1996,** *383,* 728–731.
11. Forman, B. M.; Ruan, B.; Chen, J.; Schroepfer, G. J.; Evans, R. M. The orphan nuclear receptor LXRα is positively and negatively regulated by distinct products of mevalonate metabolism. *Proc. Natl. Acad. Sci. U.S.A.* **1997,** *94,* 10588–10593.
12. Janowski, B. A.; Grogan, M. J.; Jones, S. A.; Wisely, G. B.; Kliewer, S. A.; Corey, E. J.; Mangelsdorf, D. J. Structural requirements of ligands for the oxysterol liver X receptors LXRα and LXRβ. *Proc. Natl. Acad. Sci. U.S.A.* **1999,** *96,* 266–271.
13. Song, C.; Liao, S. Cholestenoic acid is a naturally occurring ligand for liver X receptor α. *Endocrinology* **2000,** *141,* 4180–4184.
14. Russell, D. W. Nuclear orphan receptors control cholesterol catabolism. *Cell* **1999,** *97,* 539–542.
15. Repa, J. J.; Mangelsdorf, D. J. The role of orphan nuclear receptors in the regulation of cholesterol homeostasis. *Annu. Rev. Cell Dev. Biol.* **2000,** *16,* 459–481.
16. Brown, A. J.; Jessup, W. Oxysterols and atherosclerosis. *Atherosclerosis* **1999,** *142,* 1–28.
17. Lin, Y. Y.; Welch, M.; Liebermann, S. The detection of 20(S)-hydroxycholesterol in extracts of rat brains and human placenta by a gas chromatograph/mass spectrometry technique. *J. Steroid Biochem. Mol. Biol.* **2003,** *85,* 57–61.

18. Yao, Z.X.; Brown, R. C.; Teper, G.; Greeson, J.; Papadopoulos, V. 22-Hydroxycholesterol protects neuronal cells from β-amyloid-induced cytotoxicity by binding to β-amyloid peptide. *J. Neurochem.* **2002,** *83,* 1110–1119.

19. Axelson, M.; Larsson, O.; Zhang, J.; Shoda, J.; Sjövall, J. Structural specificity in the suppression of HMG-CoA reductase in human fibroblasts by intermediates in bile acid biosynthesis. *J. Lipid Res.* **1994,** *36,* 290–298.

20. Bjorkhem, I.; Reihner, E.; Angelin, B.; Ewerth, S.; Akerlund, J. E.; Einarsson, K. On the possible use of the serum level of 7α-hydroxycholesterol as a marker for increased activity of the cholesterol 7α-hydroxylase. *J. Lipid Res.* **1987,** *28,* 889–894.

21. Axelson, M.; Aly, A.; Sjövall, J. Levels of 7α-hydroxy-4-cholesten-3-one in plasma reflects rates of bile acid synthesis in man. *FEBS Lett.* **1988,** *239,* 324–328.

22. Axelson, M.; Björkhem, I.; Reihner, E.; Einarsson, K. Plasma level of 7α-hydroxy-4-cholesten-3-one reflects the activity of hepatic cholesterol 7α-hydroxylase in man. *FEBS Lett.* **1991,** *284,* 216–218.

23. Björkhem, I.; Diczfalusy, U.; Lütjohann, D. Removal of cholesterol from extrahepatic sources by oxidative mechanisms. *Curr. Opin. Lipidol.* **1999,** *10,* 161–165.

24. Lund, E. G.; Guileyaedo, J. M.; Russel, D. W. cDNA cloning of cholesterol 24-hydroxylase, a mediator of cholesterol homeostasis in the brain. *Proc. Natl. Acad. Sci. U.S.A.* **1999,** *96,* 7238–7234.

25. Björkhem, I.; Andersson, U.; Ellis, E.; Alvelius, G.; Ellegard, L.; Diczfalusy, U.; Sjövall, J.; Einarsson, C. From brain to bile. Evidence that conjugation and ω-hydroxylation are important for elimination of 24S-hydroxycholesterol (cerebrosterol) in humans. *J. Biol. Chem.* **2001,** *276,* 37004–37010.

26. Bodin, K.; Bretillon, L.; Aden, Y.; Bertilsson, L.; Broome, U.; Einarsson, C.; Diczfalusy, U. Antiepileptic drugs increase plasma levels of 4β-hydroxycholesterol in humans: Evidence for involvement of cytochrome P450 3A4. *J. Biol. Chem.* **2001,** *276,* 38685–38689.

27. Wentworth, P.; McDunn, J. E.; Wentworth, A. D.; Takeuchi, C.; Nieva, J.; Jones, T.; Bauttista, C.; Ruedi, J. M.; Gutierrez, A.; Janda, K. A.; Babior, B. M.; Eschenmoser, A.; Lerner, R. A. Evidence for antibody-catalyzed ozone formation in bacterial killing and inflammation. *Science* **2002,** *298,* 2195–2199.

28. Wentworth, P.; Nieva, J.; Takeuchi, C.; Galve, R.; Wentworth, A. D.; Dilley, R. B.; DeLaria, G. A.; Saven, A.; Babior, B. M.; Janda, K. D.; Eschenmoser, A.; Lerner, R. A. Evidence for ozone formation in human atherosclerotic arteries. *Science* **2003,** *302,* 1053–1056.

29. Zhang, Q.; Powers, E. T.; Nieva, J.; Huff, M. E.; Dendle, M. A.; Bieschke, J.; Glabe, C. G.; Eschenmoser, A.; Wentworth, P.; Lerner, R. A.; Kelly, J. W. Metabolite-initiated protein misfolding may trigger Alzheimer's disease. *Proc. Natl. Acad. Sci. U.S.A.* **2004,** *101,* 4752–4757.

30. Pulfer, M. K.; Murphy, R. C. Formation of biologically active oxysterols during ozonolysis of cholesterol present in lung surfactant. *J. Biol. Chem.* **2004,** *279,* 26331–26338.

31. Dzeletovic, S.; Breuer, O.; Lund, E.; Diczfalusy, U. Determination of cholesterol oxidation products in human plasma by isotope dilution-mass spectrometry. *Anal. Biochem.* **1995,** *225,* 73–80.

32. Breuer, O.; Björkhem, I. Simultaneous quantification of several cholesterol autoxidation and monohydroxylation products by isotope-dilution mass spectrometry. *Steroids* **1990,** *55,* 185–192.

33. Zhang, Z.; Li, D.; Blanchard, D. E.; Lear, S. R.; Erickson, S. K.; Spencer, T. A. Key regulatory oxysterols in liver: analysis as Δ⁴-3-ketone derivatives by HPLC and response to physiological perturbations. *J. Lipid Res.* **2001,** *42,* 649–658.

34. Ogishima, T.; Okuda, K. An improved method for assay of cholesterol 7-α-hydroxylase activity. *Anal. Biochem.* **1986,** *158,* 228–232.

35. Griffiths, W. J.; Liu, S.; Alvelius, G.; Sjövall, J. Derivatives Revisited: Analysis of Neutral Steroids by ESMS. *Proceedings of the 50th ASMS Conference on Mass Spectrometry and Allied Topics*; Orlando, FL, June, 2002.

36. Griffiths, W. J.; Alvelius, G.; Liu, S.; Hornshaw, M.; Sjövall, J. Analysis of Oxysterols in Brain. *Proceedings of the 52nd ASMS Conference on Mass Spectrometry and Allied Topics*; Nashville, TN, May, 2004.

37. Wang, Y.; Alvelius, G.; Liu, S.; Bodin, K.; Hornshaw, M.; Sjövall, J.; Griffiths, W. J. Steroidomics of Brain. *Proceedings of the 53rd ASMS Conference on Mass Spectrometry and Allied Topics*; San Antonio, TX, June, 2005.

38. Griffiths, W. J.; Liu, S.; Alvelius, G.; Sjövall, J. Derivatization for the characterization of neutral oxosteroids by electrospray and matrix-assisted laser desorption/ionization tandem mass spectrometry: The Girard P derivative. *Rapid Commun. Mass Spectrom.* **2003,** *17,* 924–935.

39. Griffiths, W. J.; Alvelius, G.; Liu, S.; Sjövall, J.High-energy collision-induced dissociation of oxosteroids derivatized to Girard hydrazones. *Eur. J. Mass Spectrom.* **2004,** *10,* 63–88

40. Shackleton, C. H. L.; Chuang, H.; Kim, J.; de la Torre, X.; Segura, J. Electrospray mass spectrometry of testosterone esters: Potential for use in doping control. *Steroids* **1997,** *62,* 523–529.

41. Dharmasiri, K. A. N.; Huang, Z.-H.; Watson, J. T. Derivatives for detection of anabolic ketosteroids by positive electrospray mass spectrometry. *Proceedings of the 41st ASMS Conference on Mass Spectrometry and Allied Topics*; San Francisco, CA. May, 1993.

42. Lai, C. C.; Tsai, C. H.; Tsai, F. J.; Lee, C. C.; Lin, W. D. Rapid monitoring assay of congenital adrenal hyperplasia with microbore high-performance liquid chromatography/electrospray ionization tandem mass spectrometry from dried blood spots. *Rapid Commun. Mass Spectrom.* **2001,** *15,* 2145–2151.

43. Lai, C. C.; Tsai, C. H.; Tsai, F. J.; Wu, J. Y.; Lin, W. D.; Lee, C. C. Monitoring of congenital adrenal hyperplasia by microbore HPLC-electrospray ionization tandem mass spectrometry of dried blood spots. *Clin. Chem.* **2002,** *48,* 354–356.

44. Lai, C. C.; Tsai, C. N.; Tsai, F. J.; Wu, J. Y.; Lin, W. D.; Lee, C. C. Rapid screening assay of congenital adrenal hyperplasia by measuring 17 α-hydroxyprogesterone with high-performance liquid chromatography/electrospray ionization tandem mass spectrometry from dried blood spots. *J. Clin. Lab. Anal.* **2002,** *16,* 20–25.

45. Higashi, T.; Shimada, K. Derivatization of neutral steroids to enhance their detection characteristics in liquid chromatography-mass spectrometry. *Anal. Bioanal. Chem.* **2004,** *378,* 875–882.

46. Shoda, J.; Axelson, M.; Sjövall, J. Synthesis of potential C₂₇-intermediates in bile acid biosynthesis and their deuterium-labeled analogs. *Steroids* **1993,** *58,* 119–125.

47. Brooks, C. J. W.; Cole, W. J.; Lawrie, T. D. V.; MacLachlan, J.; Borthwick, J. H.; Barrett, G. M. Selective reactions in the analytical characterization of steroids by gas chromatography-mass spectrometry. *J. Steroid Biochem.* **1983,** *19,* 189–210.

48. MacLachlan, J.; Wotherspoon, A. T. L.; Ansell, R. O.; Brooks, C. J. W. Cholesterol oxidase: Sources, physical properties, and analytical applications. *J. Steroid Biochem. Mol. Biol.* **2000,** *72,* 169–195.

49. Liu, S.; Sjövall, J.; Griffiths, W. J. Analysis of oxosteroids by nano-electrospray mass spectrometry of their oximes. *Rapid Commun. Mass Spectrom.* **2000,** *14,* 390–400.

50. Liu, S.; Sjövall, J.; Griffiths, W. J. Neurosteroids in rat brain: Extraction, isolation, and analysis by capillary column liquid chromatography-electrospray mass spectrometry. *Anal. Chem.* **2003,** *75,* 5835–5846.

51. Wheeler, O. H. The Girard reagents. *J. Chem. Educ.* **1968,** *45,* 435–437.

52. Williams, T. M.; Kind, A. J.; Houghton, E.; Hill, D. W. Electrospray collision induced dissociation of testosterone and testosterone hydroxy analogs. *J. Mass Spectrom.* **1999,** *34,* 206–216.

53. Griffiths, W. J. Tandem mass spectrometry in the study of fatty acids, bile acids, and steroids. *Mass Spectrom. Rev.* **2003,** *22,* 81–152.

54. Lütjohann, D.; Brzezinka, A.; Barth, E.; Abramowski, D.; Staufenbiel, M.; von Bergmann, K.; Beyreuther, K.; Multhaup, G.; Bayer, T. A. Profile of cholesterol-related sterols in aged amyloid precursor protein transgenic mouse brain. *J. Lipid Res.* **2002,** *43,* 1078–1085.

55. Clifton, P. M.; Noakes, M.; Sullivan, D.; Erichsen, N.; Ross, D.; Annison, G.; Fassoulakis, A.; Cehun, M.; Nestel. P.Cholesterol-lowering effects of plant sterol esters differ in milk, yoghurt, bread, and cereal. *Eur. J. Clin. Nutr.* **2004,** *58,* 503–509.

56. Fahy, D. M.; O'Callaghan, Y. C.; O'Brien, N. M. Phytosterols: Lack of cytotoxicity but interference with β-carotene uptake in Caco-2 cells in culture. *Food Addit. Contam.* **2004,** *21,* 42–51.

57. Dhar, A. K.; Teng, J. I.; Smith, L. L. Biosynthesis of cholest-5-ene-3β, 24-diol (cerebrosterol) by bovine cortical microsomes. *J. Neucochem.* **1973,** *21,* 51–60.

58. Meaney, S.; Babiker, A.; Lütjohann, D.; Diczfalusy, U.; Axelson, M.; Björkhem, I. On the origin of cholestenoic acids in human circulation. *Steroids* **2003,** *68,* 595–601.

59. Zhang, J.; Akwa, Y.; El-Etr, M.; Baulieu, E. E.; Sjövall, J. Metabolism of 27-, 25-, and 24-hydroxycholesterol in rat glial cells and neurons. *Biochem. J.* **1997,** *322,* 175–184.

60. Zhang, J.; Akwa, Y.; Baulieu, E. E.; Sjövall, J. 7α-Hydroxylation of 27-hydroxycholesterol in rat brain microsomes. *C. R, Acad. Sci. III* **1995,** *318,* 345–349.

61. Mast, N.; Norcross, R.; Andersson, U.; Shou, M.; Nakayama, K.; Bjorkhem, I.; Pikuleva, I. A. Broad substrate specificity of human cytochrome P450 46A1 which initiates cholesterol degradation in the brain. *Biochemistry* **2003,** *42,* 14284–14292.